THESIS APPROVAL

GRADUATE SCHOOL, KASETSART UNIVERSITY

Master of Science (Earth Science and Technology)

DEGREE

Earth Science and Technology — **FIELD**

Earth Science — **DEPARTMENT**

TITLE: Numerical Grid Methods for Landslide Hazard Prediction Model at Huai Mae Mhae Watershed; Chiang Dao District, Chiang Mai Province, Thailand

NAME: Mr. Kamphol Kesjinda

THIS THESIS HAS BEEN ACCEPTED BY

THESIS ADVISOR

(Associate Professor Veerasak Udomchoke, D.Tech.Sc.)

THESIS CO-ADVISOR

(Mr. Krit Won-In, Dr.Eng.)

DEPARTMENT HEAD

(Mr. Passakorn Pananont, Ph.D.)

APPROVED BY THE GRADUATE SCHOOL ON _____

DEAN

(Associate Professor Gunjana Theeragool, D.Agr.)

THESIS

NUMERICAL GRID METHODS FOR LANDSLIDE HAZARD PREDICTION MODEL AT HUAI MAE MHAE WATERSHED; CHIANG DAO DISTRICT, CHIANG MAI PROVINCE, THAILAND

KAMPHOL KESJINDA

A Thesis Submitted in Partial Fulfillment of
the Requirements for the Degree of
Master of Science (Earth Science and Technology)
Graduate School, Kasetsart University
2011

Kamphol Kesjinda 2011: Numerical Grid Methods for Landslide Hazard Prediction Model at Huai Mae Mhae Watershed; Chiang Dao District, Chiang Mai Province, Thailand. Master of Science (Earth Science and Technology), Major Field: Earth Science and Technology, Department of Earth Science. Thesis Advisor: Associate Professor Veerasak Udomchoke, D.Tech.Sc. 101 pages.

Landslide hazard prediction model at Huai Mae Mhae watershed in Chiang Dao district of Chiang Mai Province aims to establish model for mapping landslide area by numerical grid method using 30 m x 30 m finite grids over multilayers of data in the Geographic Information System (GIS). Data included were antecedent precipitation index from daily rainfall distribution and field moisture content in soil, recession coefficient of the watershed from weir at the outlet, effective soil depth that obtain from soil profiles at road cuts and related in exponential function of aspect, slope and elevation of the study area, landuse and soil strength those are analyzed by slope stability model accompanied with moisture distribution module in Weather Research and Forecasting Model (WRF) to obtain the slope stability factors, then map the landslide area of the mountainous watershed. The results revealed that most of the watershed area is in moderate degree of landslide level due to steep slope on high mountain and loamy sandy soil derived from granitic rock that exist very high water holding capacity and easily slide down the slope. Fortunately, these areas are mostly covered with dense hill - evergreen forest that their deep roots can retain high stability on slope. Area subjected to high potential landslide is covered by tea and orchard plantation due to lack of deep roots of large tree to anchorage in soil for landslide retardation. The areas that show low degree of landslide level were demarked on the gentle slope and undulating area. The antecedent precipitation index at critical level (critical API) of this area ranged between 340 to 370 millimeters in the steep slope area that cover with agricultural land use or in the high potential landslide area.

_____ _____ ____ /____ /____

Student's signature Thesis Advisor's signature

ACKNOWLEDGEMENTS

The author wishes to express his heartfelt thanks and deep gratitude to his adviser, Assoc. Prof. Dr. Veerasak Udomchoke, who motivates, encourage and support for many thing such as data collection technique, laboratory testing technique, theoretical concepts and real experience in his work. He gives his valuable time of his work to teach his experience and to guide the way to graduate.

Sincere thanks are also extended to Assoc. Prof. Dr. Weeraphol Taesombat, Dr. Krit Won-In and Dr. Kannaree Chuangcham who not act as program committee members, but also provide a lot of valuable suggestion in this thesis.

Heartfelt thanks to Miss Wanitcha Phansri, my closest friend, for her help the author to revise table, picture, graph, wording and thesis format of this manuscript.

Sincere appreciation for office of the National Research Council of Thailand (NRCT) that supported research grant and Environmental Geotechnology and Natural Disaster Research Unit of Earth Science Department, Faculty of Science, Kasetsart University for a chance to work and study.

Last but not the least, the author expresses his indebtedness to my parents and my beloved son. They acted as constant source of inspiration throughout.

Kamphol Kesjinda

May 2011

TABLE OF CONTENTS

Page

LIST OF TABLES

LIST OF TABLES (Continued)

LIST OF FIGURES

LIST OF FIGURES (Continued)

LIST OF FIGURES (Continued)

LIST OF ABBREVIATIONS

θ	=	slope angle
ϕ'	=	internal friction angle of saturated soil
ρ_s	=	wet soil density in kg m^{-3}
γ_s	=	the unit weight of saturated soil in kN m^{-3}
ρ_w	=	the density of water in kg m^{-3}
γ_w	=	the unit weight of water in kN m^{-3}
β	=	slope angle
ϕ	=	the internal friction angle of wet soil
API	=	Antecedent Precipitation Index
c'	=	cohesion of saturated soil in kN m^{-2}
C_r	=	root cohesion in N m^{-2}
C_s	=	soil cohesion under wet condition in N m^{-2}
D	=	the vertical soil depth in m
DEM	=	digital elevation model
D_w	=	the vertical height of the water table within the soil layer in m
E	=	East
FS	=	Factor of safety
g	=	gravitational acceleration
Gs	=	Specific gravity
h	=	Soil thickness in meter
h_w	=	the vertical height of the water table within the soil layer in m
kg m^{-3}	=	kilogram per cubic meter
km hr^{-1}	=	kilometer per hour
kN m^{-3}	=	kilonewton per cubic meter
Kr	=	recession coefficient
LL	=	Liquid Limit
LPI	=	Lightning Potential Index
LPI	=	Lightning Potential Index
LRF	=	Landslide Risk Factor

LIST OF ABBREVIATIONS (Continued)

m s^{-2}	=	meters per second
m yr^{-1}	=	meter per year
m	=	meter
m^2	=	square meter
mm	=	millimeter
MM5	=	the fifth-generation NCAR / Penn State Mesoscale Model
MSL	=	Mean Sea Level
N m^{-2}	=	Newtons per square meter
N	=	North
NCAR	=	the National Center for Atmospheric Research
NGD	=	Numerical Grid Method
NM	=	Northeast Monsoon Season
NOAA	=	the National Oceanic and Atmospheric Administration
OSM	=	Onset Southwest Monsoon Season
ϕ	=	Internal friction angle
PI	=	Plastic Index
P_i	=	daily rainfall amount
PL	=	Plastic Limit
REAME	=	Rotational Equilibrium Analysis of Multilayered Embankments
R^2	=	the coefficient of determination
r_u	=	water pressure in term of pore water pressure ratio
S	=	South
SI	=	Stability Index
SIM	=	Summer Intermoonsoon Season
SINMAP	=	Stability INdex MAPping
SM	=	Southwest Monsoon Season
W	=	West
WIM	=	Winter Intermonsoon Season
WRF	=	Weather Research and Forecasting
Z	=	the vertical soil depth in meter

NUMERICAL GRID METHODS FOR LANDSLIDE HAZARD PREDICTION MODEL AT HUAI MAE MHAE WATERSHED; CHIANG DAO DISTRICT, CHIANG MAI PROVINCE, THAILAND

INTRODUCTION

Landslide is natural hazard influenced from long heavy rain period and can cause violent problem on lives and properties of people who live at the foot-slope of landslide risk area. Major causes of landslide are longtime of heavy rainfall on steep-slope of hilly area, course texture of soil and rock and bared or non-forested landuse and land cover. At the time that soil on slope reaches the degree of saturation, it become critical level that decrease soil strength, then landslide occurred.

There are two main idea of landslide area and landslide risk areas, the landslide area are identified on hill-slope, but the landslide risk areas are the area subjected to landslide at the toe of slope. These areas are all risk areas for peoples and everything that concern with peoples, but magnitude of landslide depends on area of landslide that subjected to return period of occurrence (Hunt,1984). The landslide risk map is the map that the land surface were classified into zone of varying degree of hazards based on the estimated significance of causative factor which influence the stability (Anbalagan, 1992). In Thailand, many researchers had attempted to create landslide risk map by various methods such as weighting factor method (Soralump and Chotikasathien, 2007) and Landslide Risk Factor (LRF) method (Chokesomboonkul and Udomchoke, 1999) these methods are not proper to predict landslide due to the facts that weighting factor method depend on experience of the experts to classify and rating all factors whereas the landslide risk factor method depend on occurrence probability at the relevance area that used to occur landslide in the past and are not accepted to apply for all area.

This study attempts to create landslide warning model that use the application of numerical grid methods to predict rainfall, moisture content in soil from current and antecedent rainfall and slope stability of the study area, then create the zone of landslide risk for human settlement. Study area is located at Huai Mae Mhae watershed, Ban Mae Na, Chiang Dao district, Chiang Mai Province, Thailand as shown in Figure 1.

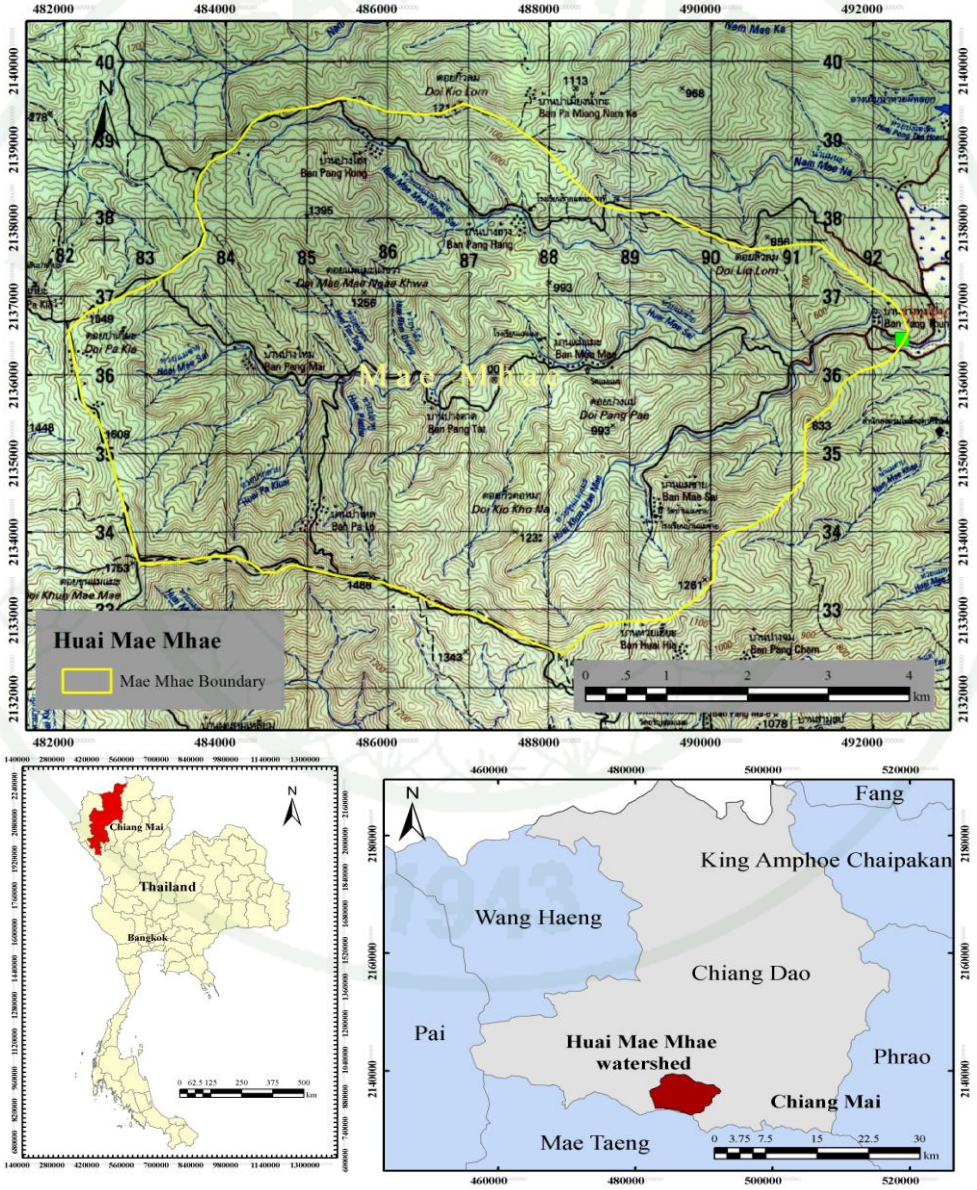

Figure 1 Topographic map of Huai Mae Mhae watershed at Ban Mae Na, Chiang Dao district, Chiang Mai Province Thailand.

OBJECTIVES

The target of this research aims to find out the landslide risk map with the objectives as follows:

1) To study the characteristics of rainfall in each particular regional weather conditions at Huai Mae Mhae watershed.

2) To create landslide model from the accompany of Numerical Grid Method (NGM) and Weather Research and Forecasting (WRF) method.

3) To comply precipitation model with landslide model and create landslide risk map.

LITERATURE REVIEW

1. Slope failure

Slope failure is the movement of mass by gravitational force. The strength of mass is equal to or greater than the gravitational force, the forces are in balance, the mass is in equilibrium and movement does not occur (Hunt, 1984). Increasing of moisture content in soils and rocks will decrease their strength, then strength of mass is larger than gravitational force and slope failure occur. Types and forms of slope failures were classified and tabulated (Table 1).

Table 1 Types and forms of slope failures.

Type	Form	Definition
Fall	Free fall	Sudden dislodgment of single or multiple blocks of soil or rock which fall in free descent.
	Topple	Overturning of a rock block about a pivot point located below its center of gravity.
Slide	Rotational or slump	Relatively slow moment of an essentially coherent block (or blocks) of soil, rock, or soil – rock mixtures along some well – defined arc – shaped failure surface.
	Planar or translational	Slow to rapid movement of an essentially coherent block (or blocks) of soil or rock along some well – defined planar failure surface.
	Subclasses	
	Block glide	A single block moving along a planar surface.
	Wedges	Block or blocks moving along intersecting planar surface.
	Lateral spreading	A number of intact blocks moving as separate units with differing displacements.

Table 1 (Continued)

Type	Form	Definition
	Debris slide	Soil – rock mixtures moving along a planar rock surface.
Avalanches	Rock or debris	Soil or soil – rock rapid movement of an incoherent mass of rock or soil – rock debris wherein the original structure of the formation is no longer discernible, occurring along an ill – defined surface.
Flows	Debris, Sand, Silt, Mud and Soil	Soil or soil – rock debris moving as a viscous fluid or slurry, usually terminating at distances far beyond the failure zone; resulting from excessive pore pressures (Sub classed according to material type)
Creep		Slow, imperceptible downslope movement of soil or soil – rock mixtures.
Solifluction		Shallow portions of the regolith moving downslope at moderate to slow rate in Arctic to sub – Arctic climates during periods of thaw over a surface usually consisting of frozen ground.
Complex		Involves combinations of the above, usually occurring as a change from one form to another during failure with one form predominant.

Source : Hunt (1984)

Landslide factors and their description were tabulated (Table 2). Velocity of movement for slope failure form was tabulated (Table 3).

Table 2 The major factors and other factors that cause landslide.

Major factors	Description
Movement form	Fall slide slide – flow (Avalanche) and flow.
Failure surface form	Arc – shaped, planar, irregular and ill – defined.
Mass coherency	Incoherent, with the original structure totally destroy. Coherent, with the original structure essentially intact although dislocated.
Constitution	Single or multiple blocks, heterogeneous mass without blocks.
Failure cause	Tensile strength or shear strength exceeded along a failure surface, hydraulic excavation, or excessive pore pressure.
Other factors	Description
Mass displacement	Amount of displacement from the failure zone, which can vary from slight to small, to very far. Blocks can move together with similar displacements or separately with varying displacements.
Material type	Rock blocks or slabs, soil – rock mixtures (debris), sand, silt, block of over - consolidated clay or mud
Rate of movement during failure	Varies from extremely slow and barely perceptible to extremely rapid (Table 3).

Source : Hunt (1984)

Table 3 Velocity of movement for slope failure forms.

Velocity ($m\ s^{-1}$)	Movement	Rate	Classification
10^{2}	Extremely rapid		
10		$3\ m\ s^{-1}$	Avalanches and flows
1	Vary rapid		
10^{-1}			
10^{-2}		$0.3\ m\ min^{-1}$	
10^{-3}	Rapid		
10^{-4}			
10^{-5}		$1.5\ m\ day^{-1}$	Slide
10^{-6}	Moderate	$1.5\ m\ month^{-1}$	
10^{-7}	Slow	$1.5\ m\ yr^{-1}$	
10^{-8}	Very slow		
10^{-9}	Extremity slow	$0.3\ m\ 5\ yr^{-1}$	Creep

Final stage (Planar slide – rock mass)

Final stage, Inter-mediate, Early stage (Rotational slide)

Source : Hunt (1984)

2. Landslides

A landslide event is defined as "the movement of a mass of rock, debris or earth down a slope" (Cruden, 1991) and the gravitational displacement of rock and soil from their normal position (Robert and Hatheway, 1988). The word 'landslide' also refers to the geomorphic features that result from the event. Other terms used to refer to landslide events include mass movements, slope failures, slope instability and terrain instability. In spite of the simple definition, landslide events are complex geological processes and are difficult to classify. The classification is based upon material type and type of movement, and is similar to the updated classification of slope movements suggested by Cruden and Varnes (1996).

A. Type of landslides

Landslides were classified into three categories (Thomson and Turk, 2007) flow, slide and fall (Figure 2 and Table 4). For example, Sand that is saturated with water will flows down the face of the structured. During flow, loose, unconsolidated soil or sediment move as fluid. Mud with high water content can flow as rapidly as water falling over a waterfall. Movement of a coherent block of material along a fracture is called slide. Slide is usually faster than flow but it until may take several second for the block to slide down the face. If one takes a huge handful of sand out of bottom, the whole tower topples. This rapid free-falling motion is called fall. Fall is the most rapid type of mass wasting. In extreme cases, like the face of a steep cliff, rock can fall at a speed dictated solely by the force of gravity and air resistance.

Table 4 Three categories of mass wasting flow, slide and fall.

Type of Movement	Description	Subcategory	Description	Comments
Flow	Individual particles move downslope independently of one another, not as a consolidated mass. Typically occurs in loose unconsolidated regolith.	Creep	Slow, visually imperceptible movement.	Trees on creep slopes are tilted down-hill and develop pistol butt shape.
		Debris flow	More than half the particles larger than sand size; rate of movement varies from less than 1 m/year to 100 km/hr or more	Common in arid regions with intermittent heavy rainfall, or can be triggered by

Table 4 (Continued)

Type of Movement	Description	Subcategory	Description	Comments
		Earth flow and mudflow	Movement of fine-grained particles with large amounts of water.	volcanic eruption
Slide	Material moves as discrete blocks; can occur in regolith or bedrock	Earth flow and mudflow	Movement of fine-grained particles with large amounts of water.	
		Rockslide	Usually rapid movement of a new detached segment of bedrock.	
Fall	Material fall freely in air typically occurs in bedrock	-	-	Occurs only on steep cliffs.

Source : Thomson and Turk (2007)

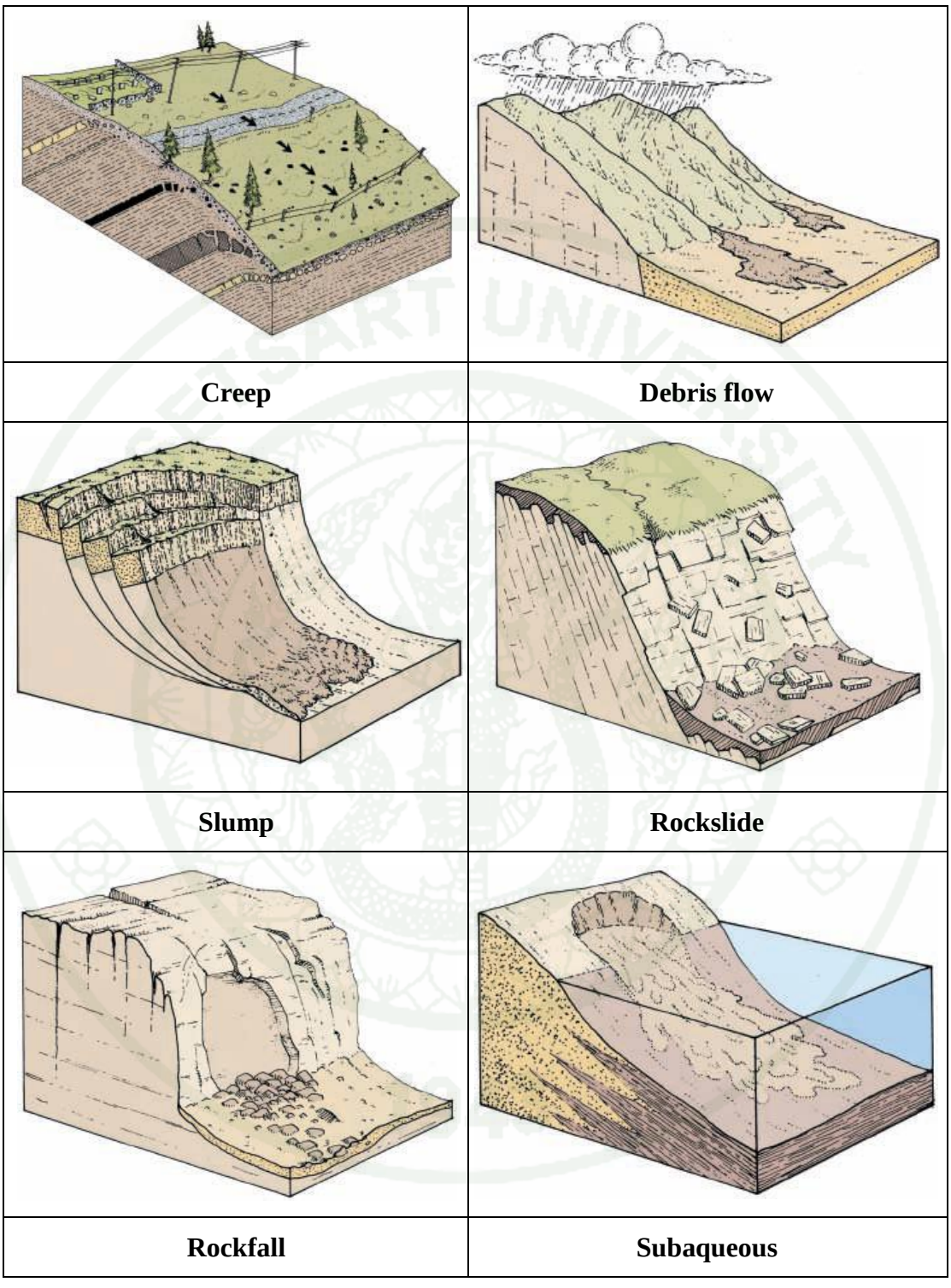

Figure 2 The categories of mass wasting flow, slide and fall.

Source: Hamblin and Christiansen (2003)

B. Cause of landslides

Landslides are caused by either the decreased ability of a slope to resist gravitational influence, an increased effectiveness of gravity acting on the slope, or a combination of these two elements. Some causes are inherent or basic condition, the nature of the bedrock or soil present, topography, vegetation and climate (Varnes, 1984). Other causes are due to more transitory conditions that produce changes, either increasing stress or decreasing material strength. Among these conditions are vibration from earthquake motion, fluctuating groundwater level and the reshape of slope by man. Changing the slope at this susceptible location initiated the current landslide problems. Probably the most important stability control factor is change in groundwater control conditions. This may be caused by interference with natural drainage conditions, excessive evaporation from normally damp ground, or an increase in groundwater level due to excessive rainfall. When surface erosion strips off vegetation and bares the ground to rainfall infiltration, this may lead very quickly to an increase in groundwater and its three negative effects (Robert and Hatheway, 1988) (1) an increases of the effective weight of the material that it saturates (2) buildup of pore pressure and (3) weakening of many materials, including weak rock and unconsolidated material with any clay content. One or more of these effects combined with the consequences of heavy rainfall will explain why many slides occur in wet weather and why internal and external drainage is so often an effective remedy for sliding.

Jotisankasa and Sawangsuriya (2008) presented the theory of unsaturated soil mechanics and some related studies that carried out in Thailand including laboratory tests and field monitoring numerical analysis on their applications for quantitative assessment of slope performance. Understanding of soil behavior in unsaturated state and any changes in its characteristics due to saturation or evapotranspiration will enable engineers to predict the actual slope behavior in the field. The important characters include shear strength variation with suction swelling, shrinkage or collapse due to suction change as well as seepage and water retention capacity.

Prasertying (2008) analyzed rainfall characteristic that cause landslide from recorded of the meteorological station in landslide areas at Muang district, Chanthaburi Province. Landslide hazard occurred on 30 July, 1999 due to rainfall amount as 137.9 millimeter during the central pattern of rainfall. The landslide at Banphongern, Muang District, Phetchabun Province on 11 September, 2000 due to rainfall amount as 121.1 millimeters during the central pattern of rainfall. Landslide at Wangchin District, Phrae Province on 4 May, 2001 by rainfall amount as 285.5 millimeters during the delayed pattern of rainfall. Landslide at Muang District, Phrae Province on 23 May, 2006 due to rainfall amount as 110.0 millimeters during the central pattern of rainfall. From this study on rainfall pattern implied that the central patterns of rainfall amount greater than hundred millimeters may cause landslide on the steep hillslope.

3. Hazard and risk degree

An existing or potential slope failure must be evaluated in terms of the degree of the hazard and the risk degree (Table 5) when hazard refers to the slope failure in terms of its potential magnitude and probability of occurrence, but risk refers to the consequences of failure on human activities (Table 6).

Table 5 Criteria of hazard degree area.

Hazard Degree	Description
No Hazard	A slope is not likely to undergo failure under any foreseeable circumstances.
Low Hazard	A slope may undergo total failure under extremely adverse conditions which have a low probability of occurrence, or potential failure volume and area affected are small even though the probability of occurrence is high.

Table 5 (Continued)

Hazard Degree	Description
Moderate Hazard	A slope probability will fail under severe condition which can be expected to occur at some future time, and a relatively large volume of material is likely to be involved. Movement will be relatively slow and the area affected will include the failure zone and a limited zone downslope (moderate displacement).
High Hazard:	A slope is almost certain to undergo total failure in the near future under normal adverse conditions and will involve a large to very large volume of materials, or a slope may fail under severe conditions, but the potential volume and area affected are enormous, and the velocity of movement very high.

Source : Hunt (1984)

Table 6 Criteria of landslide risk area.

Risk Degree	The consequences of failure
No Risk	The slope failure will not affect human activities.
Low Risk	An inconvenience easily corrected, not directly endangering lives or property, such as a single block of rock of small size causing blockage of a small portion of roadway and easily avoided and removed.
Moderated Risk	A more severe inconvenience, corrected with some effort, but not usually directly endangering lives or structures when it occurs, such as a debris slide entering one lane of a roadway and causing partial closure for a brief period until it is removed.

Table 6 (Continued)

Risk Degree	The consequences of failure
High Risk	Complete loss of roadway or important structure, or complete closures of a roadway for some period of time, but lives are not necessarily endangered during the failure.
Very High Risk	Lives are endangered at the time of failure by that it has no time for a warning.

Source : Hunt (1984)

4. Landslide Hazard Map

Organization of American States (1991) stated that a landslide hazard map is map to identify areas of differing landslide potential may be generated. The degree of landslide hazard is considered since it represents the expectation of future landslide occurrence based on the conditions of that particular area. Another area may appear similar, but may have a differing landslide hazard due to a slightly different combination of landslide conditions. Landslide susceptibility is related to the conditions of each specific area, and it cannot be assumed to be identical for a similar appearing area. Even with detailed investigation and monitoring, it is extremely difficult to predict landslide hazards in absolute terms. Sufficient understanding of landslide processes does exist, however, to be able to make an estimation of landslide hazard potential.

A. Landslide Hazard Mapping

Interpretation of future landslide occurrence requires an understanding of conditions and processes controlling landslides in the study area. Three physical factors, slope steepness, and depth of bedrock, are the minimum components necessary to assess landslide hazards. It is also desirable to add a hydrologic factor to reflect the important role which ground water often plays in the occurrence of

landslides. An indication of this factor is usually obtained indirectly by looking at vegetation, slope orientation, or precipitation zones. All of these factors are capable of being mapped. Specific combinations of these factors are associated with differing degrees of landslide hazards. The technique used to prepare hazard maps is called a combined factor analysis.

There are four steps to analysis the factor and produce a hazard map: (1) map the existing landslides and prepare a map combining the permanent factors (bedrock, slope steepness, and, when available, the hydrologic factors) into individual map units, (2) overlay the landslide inventory on the combined factor map, (3) prepare a combined factor analysis for all combinations of the factors and group combinations of these factors in a way that defines the four levels of landslide hazard and (4) produce a map with four landslide hazard zones from the grouped combinations.

B. Interpreting Landslide Hazards: The Landslide Hazard Map

A landslide hazard map is generated to identify areas with differing landslide hazards. A hazard map is produced for each stage of the planning process, from the more generalized map in the initial stage to a detailed zonation map for specific site use. The landslide hazard map is produced by interpreting the data represented by the maps of the inventoried landslides and the permanent factors found to influence the occurrence of landslides.

Four levels of relative hazard are identified on a landslide hazard map: (1) low, (2) moderate, (3) high and (4) extreme hazard. The level of landslide hazard is measured on the ordinal scale with this method and is a quantitative representation of differing hazard levels that shows only the order of relative hazard at a particular site and not absolute hazard. Predicting absolute hazard is impractical with current capabilities.

Chokesomboonkul and Udomchoke (1999) generated landslide risk map of Pak Phanang Watershed Nakhon Sri Thammarat Province from the basis of Landslide Risk Factor (LRF) method those depended on the occurrence probability at the area that used to occur landslide in the past. Their map was created in the GIS form that quite fit with real landslide area.

Soralump and Chotikasathien (2007) used geotechnical engineering method and weighting factor method to make landslide hazard map in Thailand. Various factors that indicated landslide potential were considered in the analyses including the new factor from geotechnical engineering properties of residual soil such as strength reduction. In order to include this factor in the hazard mapping analysis, appropriate laboratory testing was designed to determine the properties that can indicate the landslide potential of each type of residual soil. As for rainfall factor, the daily rainfall accumulations of various return periods were used instead of using the average rainfall intensity or annual rainfall precipitation. Various landslide hazard maps were produced based on 3 days accumulated rainfall of different return period used for analyses. GIS tool was used for map making.

5. Slope Stability Programs

A. The SINMAP (Stability INdex MAPping)

The SINMAP method was presented in term of infinite slope stability model (Hammond *et al*., 1992; Montgomery and Dietrich, 1994) that balances the destabilizing components of gravity and the restoring components of friction and cohesion on a failure plane parallel to the ground surface with edge effects neglected. SINMAP derives its terrain stability classification from inputs of topographic slope and specific catchments area and from parameters quantifying material properties (such as strength) and climate (primarily a hydrologic wetness parameter). Each of these parameters is delineated on a numerical grid over the study area. The primary output of this modeling approach is a stability index, the numerical value of which is used to classify or categorize the terrain stability at each grid location in the study

area. The topographic variables are automatically computed from digital elevation model (DEM) data. The other inputs parameters are recognized to be uncertain so are specified to SINMAP in terms of upper and lower bounds on the ranges they may take.

The stability index (SI) in SINMAP is defined as the probability that a location is stable assuming uniform distributions of the parameters over these uncertainty ranges. Where the most conservative (destabilizing) set of parameters in the model still results in stability, the stability index is defined as the factor of safety (ratio of stabilizing to destabilizing forces) at this location under the most conservative set of parameters. SINMAP uses the term ‘defended slope’ to characterize regions where, according to the model, the slope should be unstable for any parameters within the parameter ranges specified. These components are combined with an accounting for parameter uncertainty to define the stability index SI (table 7).

Table 7 Slope stability Class Definitions and criteria.

Condition	Class	Predicted State	Parameter Range	Possible Influence of Factors Not Modeled
1.5 < SI	1	Stable slope zone	Range cannot model instability	Significant destabilizing factors are required for instability
1.25 < SI < 1.5	2	Moderately stable zone	Range cannot model instability	Significant destabilizing factors are required for instability
1.0 < SI < 1.25	3	Quasi-stable slope zone	Range cannot model instability	Minor destabilizing factors could lead to instability

Table 7 (Continued)

Condition	Class	Predicted State	Parameter Range	Possible Influence of Factors Not Modeled
0.5 < SI < 1.0	4	Lower threshold slope zone	Pessimistic half of range required for instability	Destabilizing factors are not required for instability
0.0 < SI < 0.5	5	Upper threshold slope zone	Optimistic half of range required for stability	Stabilizing factors may be responsible for stability
SI < 0.00	6	Defended slope zone	Range cannot model stability	Stabilizing factors are required for stability

Source : Pack *et al.* (2005)

Thiebes *et al.* (2007) used GIS-based approach to model spatial susceptibility of shallow landslides and has been applied to a study area in southwestern Germany. The implemented model SINMAP is based on the 'infinite-slope stability model'. Different spatial scales of input data ranging from 1 m to 100 m were used to identify appropriate spatial resolutions. Validation was conducted with a landslide inventory map. Results show a high proportion (75-82%) of shallow translational landslides in the areas modeled as most susceptible. Further on, an analysis of model sensitivity to modification of geotechnical parameters was carried out, which displayed a strongly varying influence.

Theory basis for SINMAP : The Infinite Slope Stability Model (Figure 3).

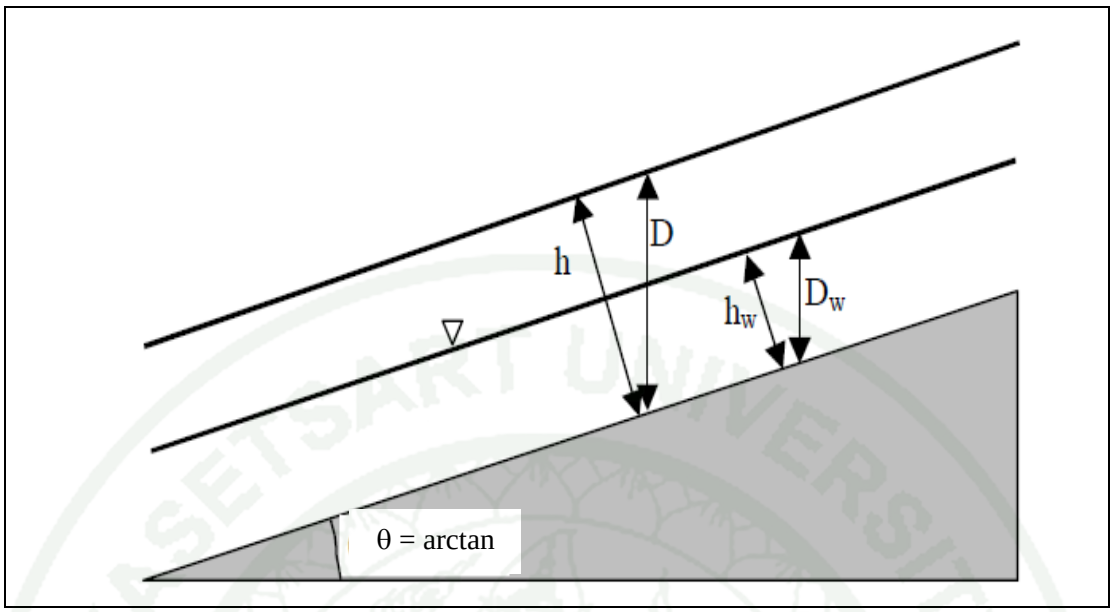

Figure 3 Infinite slope stability model schematic.

Slope stability factor (FS) for debris flow of infinite slope and bare saturated soil can be calculated as show in (1)

$$FS = \frac{c'+(\gamma_s.Z - \gamma_w.h_w)\cos^2\beta.\tan\phi'}{\gamma_s.Z.\sin\beta.\cos\beta} \quad (1)$$

Where;

	c'	is cohesion of saturated soil (kN m^{-2})
	ϕ'	is internal friction angle of saturated soil
	β	is slope angle
	Z	the vertical soil depth (m)
	γ_s	the unit weight of saturated soil (kN m^{-3})
	γ_w	the unit weight of water (kN m^{-3})
	h_w	the vertical height of the water table within the soil layer (m)

The infinite slope stability model for factor of safety at the area of trees coverage is given by simplified for wet and dry density (Hammond *et al.*, 1992).

$$FS = \frac{C_r + C_s + \cos^2\theta[\rho_s g.(D - D_w) + (\rho_s g - \rho_w g).D_w]\tan\phi}{D\rho_s g.\sin\theta.\cos\theta} \quad (2)$$

Where;

C_r is root cohesion (N m^{-2})

C_s is soil cohesion under wet condition (N m^{-2})

θ is slope angle

ρ_s is wet soil density (kg m^{-3})

ρ_w is the density of water (kg m^{-3})

g is gravitational acceleration (9.81 m s^{-2})

D the vertical soil depth (m)

D_w the vertical height of the water table within the soil layer (m)

ø the internal friction angle of wet soil

The slope angle θ is the arc tangent of slope (S) expressed as a decimal drop per unit horizontal distance. The hydrologic model is applied to interpret soil thickness as specified perpendicular to the slope, rather than soil depth measured vertically. Soil thickness, h (in meter), and depths as

$$h = D\cos\theta \quad (3)$$

B. The KU slope

The KU slope is a Slope Stability Program that developed from REAME program (Rotational Equilibrium Analysis of Multilayered Embankments) of Dr. Yang H. Huang, P.E. by Kasetsart University and at present it has been continuously developed. The theory of stability analysis in KU slope is the ordinary method of slices, or Fellenius' Method (in 1927) and the Simplified Bishop Method (in 1955).

The Ordinary Method of Slices or Fellenius' Method has developed by Fellenius (1927), the soil mass above the failure surface is subdivided into vertical slices, and the stability is calculated for each individual slice. Fellenius' Method simplifies the equation by assuming that the forces acting on the sides of each slice cancel each other. While this enables a solution to be determined, the assumption is not completely correct, and leads to low values for the computed factor of safety. In 1955, Bishop refined the method of slices technique by accounting for the interslice normal forces, thus calculating the Factor of Safety with increased accuracy. The method of slices he developed is known as the Simplified Bishop Method.

KU slope analysts slope failure base on the movement of surface failure which is circular slips. KU slope can specifies the multi-layered of soil that has difference property and determine the effects by water pressure in term of pore water pressure ratio (r_u) and phreatic surface include the effects by horizontal seismic coefficient that uses pseudo-static. When calculate safety of factor it can be specified a center of failure and this program has worked automatically to find the center of failure by grid method.

6. Numerical grid methods

Numerical grid is a finite set of points that distributed over a calculation field. This field may be a surface of the points that form triangular, quadrilateral or hexagonal cells. The field is a spatial domain the points that can be defined as tetrahedral or hexahedral cells.

Keller (1968) and Smith (2003) stated the same ideas that there were two types of numerical grid methods; finite difference and finite element method. Finite difference method is the simply interactive of small equal difference those are related to gathers with the difference from Taylor's series. Finite elements methods is the method those relate together between triangular nodes and another set of triangular nodes to form surface or volume of the interested problem. Boundary values are very import factors of both methods.

7. Weather Research and Forecast (WRF) Model

The WRF model is the second generation mesoscale model such as MM5 which is the latest numerical program model in weather simulation model. It is developed by the accompany between the National Oceanic and Atmospheric Administration (NOAA), the National Center for Atmospheric Research (NCAR), and more than 150 other organizations and universities in the United States and abroad (The National Center for Atmospheric Research, 2006).

The WRF model is a flexible model that support many type of weather parameter in prediction or forecasting. These parameters included in WRF version 2.2 are real-data and idealized simulations, various lateral boundary condition options for real-data and idealized simulations, full physics options, positive-definite advection scheme, non-hydrostatic and hydrostatic (runtime option), one-way, two-way nesting and moving nest, three-dimensional analysis nudging, and observation nudging

Lynn and Yair (2010) used WRF model for Prediction of lightning flash density in term of Lightning Potential Index (LPI) which are of the potential for charge generation and separation those leads to lightning flashes in convective thunderstorms. It was designed to predict the potential of lightning occurrence in operational weather forecasting models. The index is used grid-scale transparent between 1 and 4 km. From this research, maps of LPI and predicted lighting density was produced in regular operational runs of short range forecasting models and to serve as a valuable early warning tool for relevant users.

Inthacha *et al.* (2004) used WRF model to the track of the Chanthu depression in South China Sea westward to Thailand during June 10-15, 2004. From his research, maximum precipitation amounts in Phitsanulok on June 14, 2004 about 60-120 mm were simulated by WRF model while observed maximum precipitation amounts were 121.1 mm. The natural hazard from Chanthu depression that caused heavy rainfall was well agreed with the reported severe flood in Phitsanulok province and nearby areas.

8. Antecedent Precipitation index (API)

The Antecedent Precipitation Index (API) is a simple number derived from rainfall depth, which can be compared with or used to estimate soil moisture. The goal of this activity is to develop quantitative skills that will allow one to analyze soil moisture based on a simple model of rainfall storage and evaporation (Linsley *et al.*, 1988).

Lehmann and Holzmann (2008) combined API storage concept for flood warning level forecasting in ungauged catchments. The Antecedent Precipitation Index (API) as a possible variable to estimate runoff warning classes. The aim was to define API warning classes which correspond to runoff warning classes at a certain runoff gauge and apply the method to ungauged basins. To consider time and state dependant rainfall losses a spatially distributed linear storage concept was applied to intercept the actual rainfall. Finally, all parameter and API index was combined together and produced in iso-height of risk map.

Ornarsa *et al.* (2010) used API index in Flood warning model for Nam Khor Watershed, Lomsak district, Petchabun province from collected data during 2001 and 2006 indicated that the amounts of the rainfall varied with elevation with an annual average of 1,582.8 mm and stream flow potential of 23.3×10^6 m^3. Finally, the chance of floods to occur was then divided into normal, warning, risky and critical levels.

9. Mountainous Soil and Geology

Geology of the high mountain in northern Thailand is mostly granite due to the tectonic activity during Shan Thai and Indochina Suture during late Triassic as reported by Bunopas and Vella (1978) and confirmed by Phisit *et al.* (1992).

Intension of magma to the overlain sedimentary rocks caused metamorphic contact and isothermal activity as well as faulting and folding of these rocks. During time elapsed from late Triassic to present, remnant of the overlain rock occurred at the

outer rim of the mountain range whereas the inner most are granite and accompanied. The highest level watersheds are mostly in granitic zone whereas the lower head watershed those located on the outer rings are metamorphic rocks to sedimentary rocks of Silurian and Devonian to Carboniferous to Permian age respectively as referred by Udomchoke and Mingthipol (1995).

Soil on the high mountain those derived from granitic rocks, properties of soils, thickness of profiles, aspect and elevation of sampling points from six locations of granite from Carboniferous to Triassic age carried out and reported. Granite Feldspar, biotite and muscovite are the major minerals both in carboniferous granite and Triassic granite. Sandy clay loam to loam are the major texture of soils in the study areas especially for A profile and B profile with that depths range between 2.5 to 6 m depending on their elevation and aspect. Total porosity of those granitic soils range between 46 to 50 percent as well as 5 to 8 percent of organic matter those cause their density slightly less than 1.5 grams per cubic meter. Pore-size distribution of mountainous soil derived from gneiss at Doi Pui Chaingmai 75 kilometers southwest from Mae-Mhae watershed were studied by Udomchoke (1981). He reported that total porosity of this sandy clay loam soil range between 50 to 63 % with about 22 to 25 % range in non-useful pores (< 19 µm), 8 to 10 % range in the available water content pores (0.19 to 9 µm), 6 to 8 range in the slow drain pores (9 to 30 µm), 5 to 8 % range in the fast drain pores (60 to 120 µm), 9 to 10 % range in the vary fast drain pore (> 120 µm) respectively.

Anongrak (1989) carried out his research on the genesis of highland soils derived from granitic rocks in the Upper North of Thailand and concluded that the mineral composition of dark grayish brown porphyritic granite at Ban Kae Noi (coordinate ^{4}635E, ^{21}796N map sheet 4748II, L7018 about 30 km north of Ban Mae Na, Chiangdao district, comprises of quartz (31.8%), plagioclase (28.9%), alkali feldspar (21.9%), biotite (17.3%), Zircon (0.1%) and apatite (0.1%). These mineral compositions derived to sandy clay loam texture after completely weathered, but become coarse sandy loam soil or weathering grade V at C profile. Incompletely weathered plagioclase, alkali feldspar, biotite and quartz conduct disintegrated coarse

grained of these minerals. These disintegrated minerals caused very low cohesion as well as very low internal friction angle due to lack of clay mineral as well as broken grain of quartz, plagioclase, alkali feldspar and biotite.

MATERIALS AND METHODS

Materials

1. Geologic maps scale 1:50,000 by Department of Mineral resources.
2. Topographic maps scale 1:50,000 by Royal Thai Survey Department.
3. Land Used/Land Cover Maps scale 1:500,000.
4. Image satellite (Landsat 5, 7) scale 1:50,000.
5. Soil maps scale 1:50,000 by Land Development Department.
6. Data Processing
   6.1. Computer hardware
      - Desktop computer that has math coprocessor
      - Notebook computer
      - Hard disk drive 200 GB
      - Monitor and system control
      - Laser printer and Ink jet color printer A4 size
      - Scanner
      - Digital camera
   6.2. Software program
      - Microsoft Office
      - Quantum GIS/Arcview
7. Office stationary.
8. Weather Research and Forecasting (WRF) Model.
9. Field direct shear apparatus such as 0.28 m ×0.28 m shear box, dial gage, proving ring, rotary jack hammer.
10. Soil core and box sampling.
11. Moisture tension apparatus with 3 bar plate, cooker chamber and pressure control meter.
12. Tipping bucket recording rain gauges in data loggers.
13. Three steps rectangular weir and 120°V-notch weir with automatic recording water level by data loggers as shown in Appendix figure 1 and 2.

Methods

Step of work in this research were compiled as shown in Figure 4 and were tabulated in Table 8.

1. Engineering geological mapping of Huai Mae Mhae Watershed, Chiang Dao District, Chiang Mai Province, Thailand was carried out.

2. Disturbed and undisturbed soil samples were collected from specific of soil and rock unit in order to carry out testing in laboratory. Engineering soil properties of soil samples were tested as follow the American Standard of Testing Materials (ASTM) as follow:

2.1 Moisture content (W_n) follows ASTM D2216 – 98

2.2 Unit weight (γ_t) follow ASTM D7263 – 09

2.3 Specific gravity (G_s) follows ASTM D854 – 98

2.4 Atterberg's Limit follows ASTM D4318 – 98

2.5 Soil moisture characteristic curve follow ASTM D6836 – 02

2.6 Suction – moistured unconfined compression test follow ASTM D2166 – 98a

3. Field direct shear test were carried out from each specific soil unit that susceptible to slide from steep slope. Field direct shear apparatus comprised of shear box (0.28 m × 0.28 m × 0.14 m), proving ring and rotational jack hammer as shown in Figure 5.

4. Field soil moisture were weekly collected from specific site at Ban Pang Mai, Ban Mae Sai and Ban Mae Mhae.

5. Install tipping bucket (digital recording) rain gauge at ridge top, hillslope and at the footslope of the hill in order to calculated rainfall intensity and daily rainfall amount (P_i) of this area. Antecedent precipitation Index (API) for each successive day were calculated from recession coefficient (Kr) of the watershed as refered from Linsley et al (1988) as shown in equation (4)

$$API = K(API_{i-1}) + P_i \quad (4)$$

6. Establish numerical grid model to compile rainfall data with WRF and come out with API, then input in Quantum GIS and Arcview geographic Information System and calculate the slope stability map.

7. Landuse, soil properties in each geological unit, slope, aspect, elevation were numerically grid prepared, the calculated effective depth and critical API for slope stability calculation.

8. Input and output landslide factors in term of topography, rainfall intensity, landuse, geology, soil, API, effective depth and factor of safety as shown in Table 8.

9. Numerical grid model were established to calculate slope stability factor from equation (2).

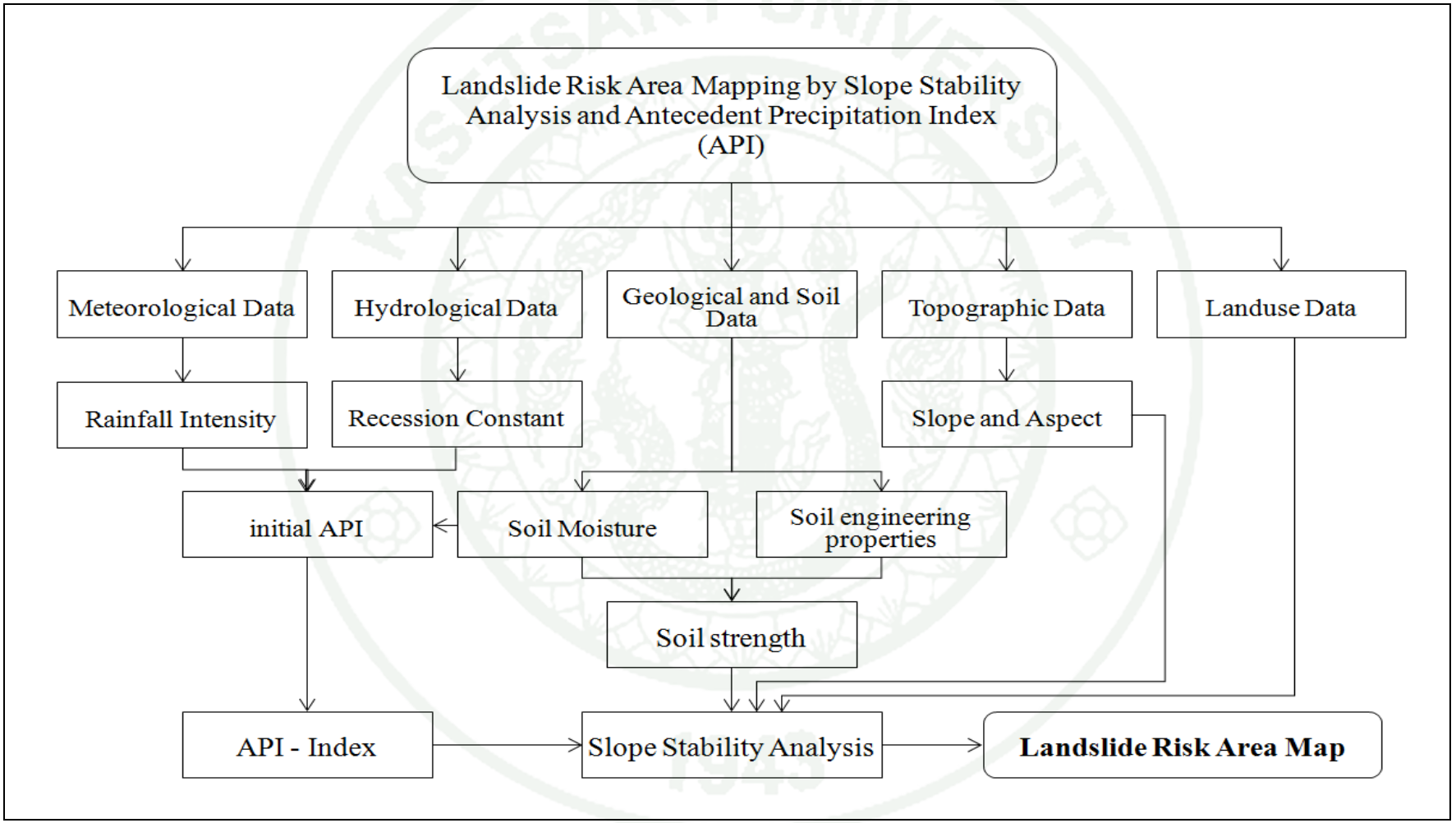

Figure 4 Flow chart of the method of study on numerical grid methods on landslide hazard prediction.

Table 8 Input and output of landslide factor for numerical grid calculation on slope stability.

Factors	Input	Output
Topographic	- Digital Elevation Model (DEM)	Topographic factor map
- Slope	- Digital Elevation Model (DEM)	Slope factor map
- Aspect	- Digital Elevation Model (DEM)	Aspect factor map
Rainfall Intensity	- Annual rainfall data	Isohyet of rainfall distribution
Landuse	- Landuse data - Field data	Landuse factor map
Geology	- Geological map - Field data	Geological factor map
Soil	- Soil map - Field data	Soil factor map
Antecedent Precipitation Index (API)	- Soil moisture at depth 15, 35 55 and 100 cm - Daily rainfall data from 7 stations - Soli depth	Soil moisture factor map
Effective Depth	- Runoff data - Rainfall data	Effective depth factor map
Factor of safety (FS)	- Property of soil mechanic	Factor of safety map

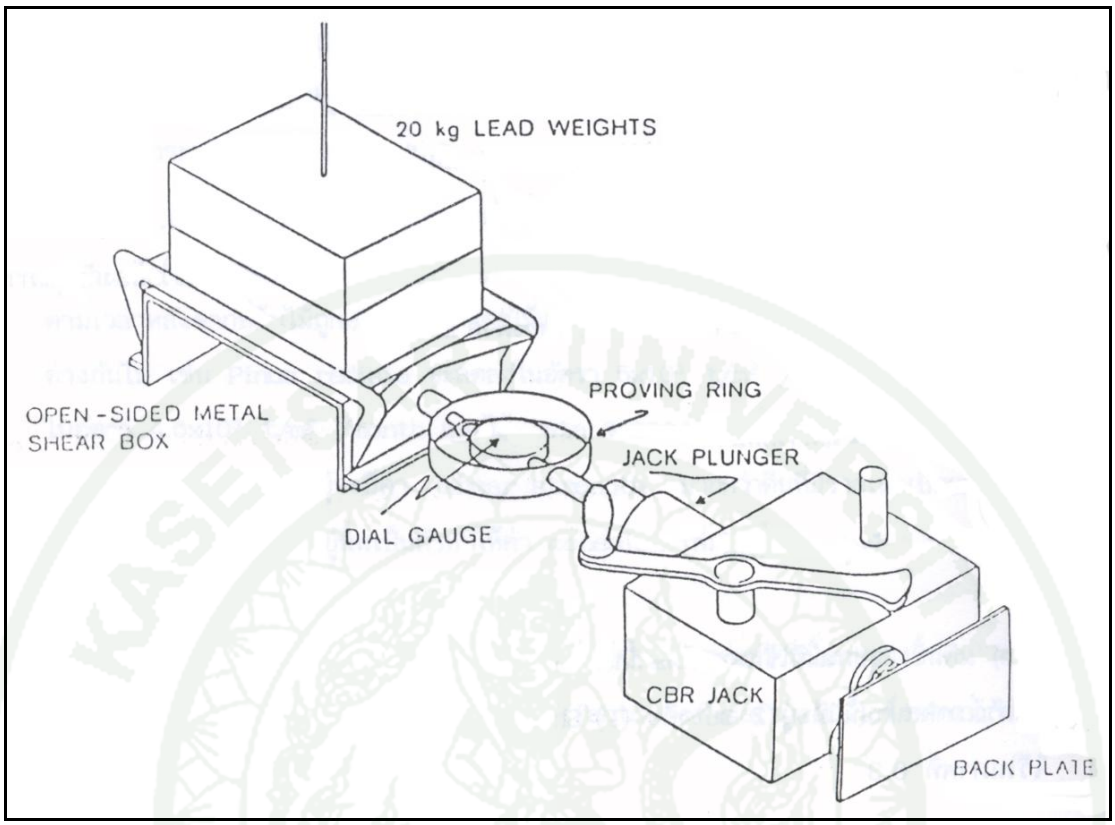

Figure 5 Set of Field direct shear apparatus comprise of open – sided metal shear box (0.28 m × 0.28 m × 0.14 m), proving ring and rotational jack hammer.

Source: Tangtam *et al.* (1994)

RESULTS AND DISCUSSION

Targets of this research aimed to use numerical grid method for creating landslide map accompanied with Weather Research and Forecasting (WRF) model to obtain the threshold level of antecedent precipitation index for landslide triggering. Results of the research are as follow:

1. Physiographic Characteristics

Huai Mae Mhae watershed is a subwatershed of Mae Ping watershed. It locates at Ban Mae Mhae, Chiang Dao district, Chiang Mai Province. Area of Huai Mae Mhae watershed is 46.57 km^2 and altitude from footslope to ridge top range between 200 to 2,000 meters from mean sea level (MSL). Main stream of the watershed flow from west to east direction and compose of 1^{st} to 4^{th} stream order. The outlet of stream locates at co-ordinate 2,136,454N, 492,363E at the rolling topography of Huai Mae Mhae watershed as shown in Figure 6.

Topography of Huai Mae Mhae watershed comprises of steep slope high mountain that cover with hill evergreen forest, hill and undulating area under the dry dipterocarp forest coverage and paddy field or rice field on the alluvium of upper Ping River basin. Seventy percent of slope of Huai Mae Mhae watershed is greater than 35 percent slope. Areal distribution in each range of elevation from less than 500 m MSL, 501 to 750 m, 750 to 1,000 m, 1,001 to 1,200 and greater than 1,200 are 0.1, 12.9, 28.5, 24.7 and 23.7 percent respectively as shown in Table 9 and Figure 7. These elevation distributions imply that nearly 42% of watershed area situate at the elevation less than 1,000 m MSL.

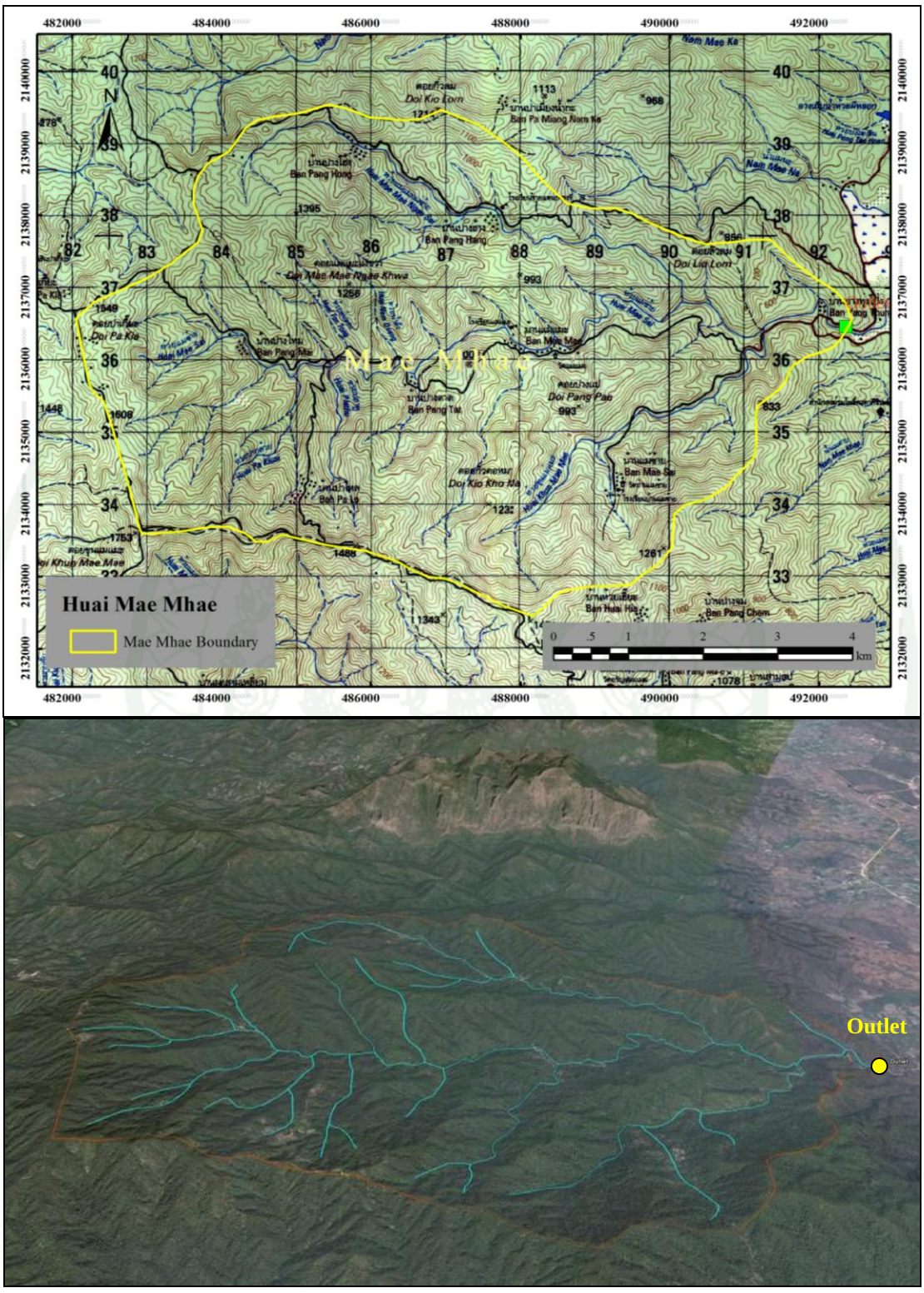

Figure 6 Topographic map series L7018 sheet 4747 I (upper) and scenery map (lower) of Huai Mae Mhae watershed, Chiang Dao district, Chiang Mai Province.

Table 9 Distribution of percent area in each elevation range of Huai Mae Mhae watershed.

Elevation (m)	< 500	501 – 750	751 – 1,000	1,001 – 1,250	> 1250
Area (km^2)	0.06	6.05	13.28	16.16	11.06
Percent	0.1	12.9	28.5	34.7	23.7

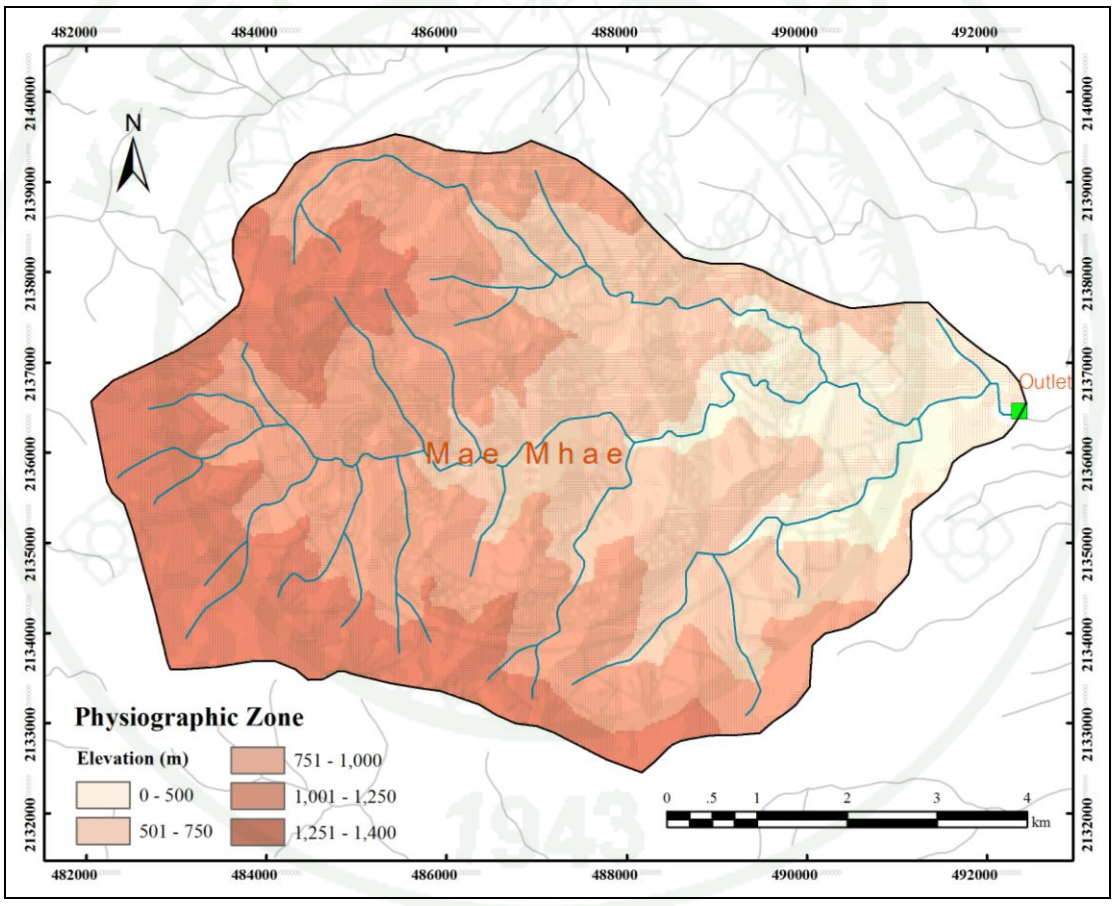

Figure 7 Physiographic zone of Huai Mae Mhae watershed exist in each range of elevation.

The watershed area oriented in the north aspect (N, NE and NW) about 35.3% in south aspect (S, SE and SW) about 36.6% and in the east and west aspect about 21.9% and 5.3% respectively as shown in Table 10 and Figure 8.

Table 10 Spatial distribution of aspect in percent area that oriented in eight directions.

Aspect	N	NE	E	S-E	S	S-W	W	N-W
Area (km^2)	8.31	0.96	8.30	6.75	4.14	3.00	2.02	1.52
Area (%)	21.9	2.5	21.8	17.8	10.9	7.9	5.3	11.9

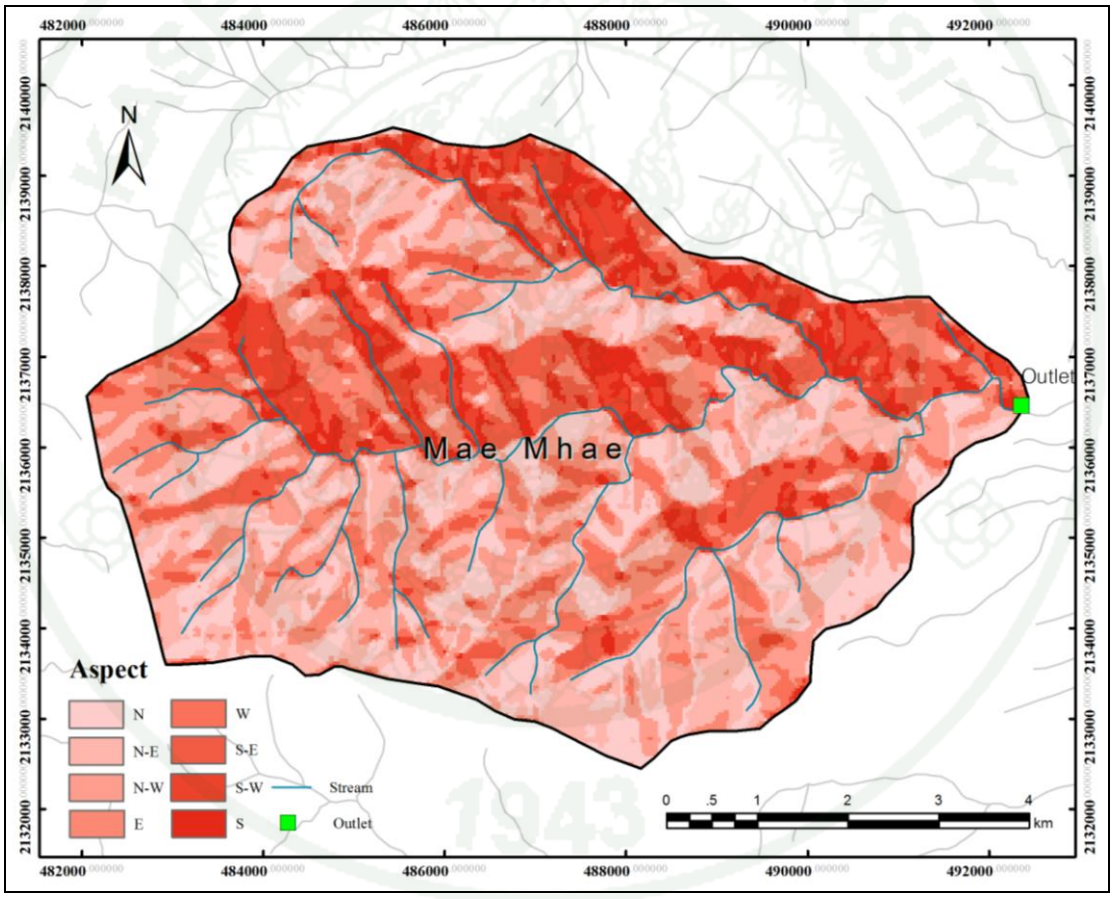

Figure 8 Spatial distribution of aspect in Huai Mae Mhae watershed.

More than 87.7% of total watershed area exist on the slope between 9 to 35 degree or 16% to 70% as shown in Table 11 and Figure 9. About 53.4 percent of total watershed area located on the steep slope (36 – 70%) and located on gentle to slightly

steep slope (34.3 %) and lower than the threshold level of hill evergreen forest (16 – 35%) and greater the 1.3% located on the very steep slope.

Table 11 Distribution of slope in percent and degree at Huai Mae Mhae watershed.

Slope (degree)	0 - 3	4 - 8	9 - 16	17 - 35	> 36
Slope (%)	0 - 5	6 - 15	16 - 35	36 – 70	> 70
Area (km^2)	0.64	4.46	16.04	24.93	0.60
Area (%)	1.4	9.6	34.3	53.4	1.3

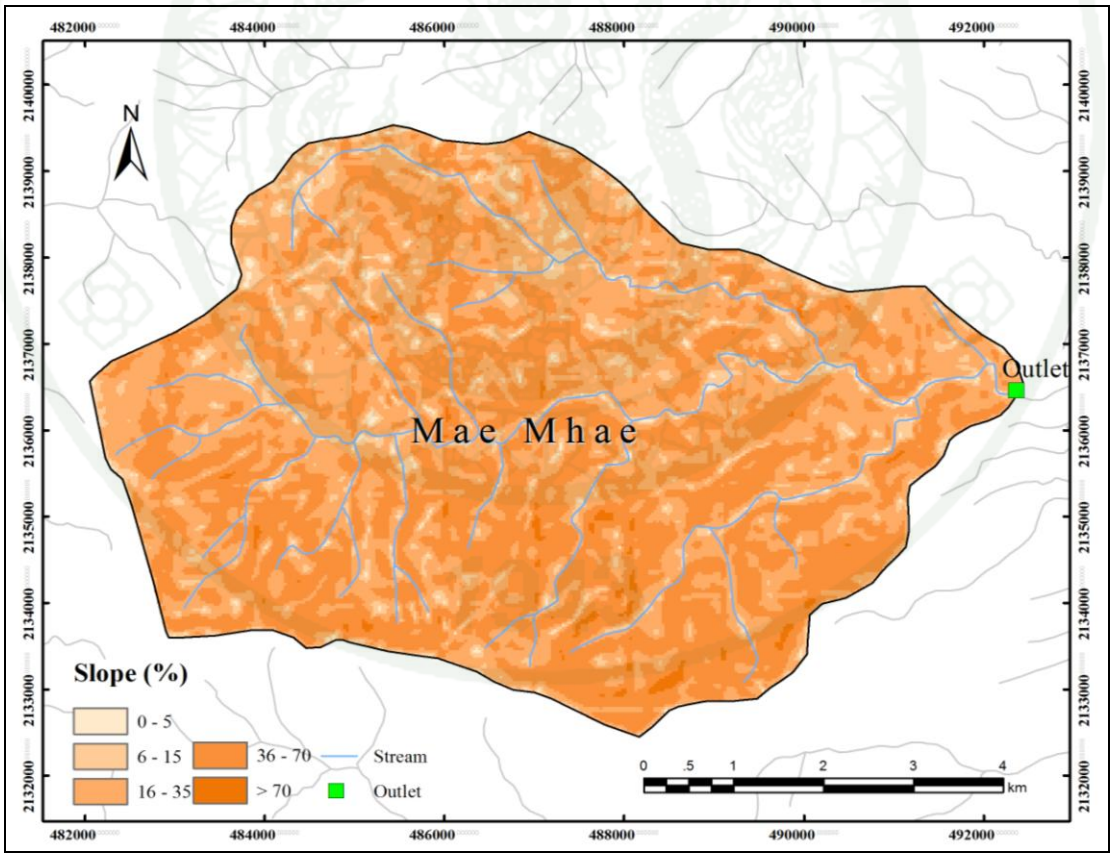

Figure 9 Areal distribution of slope in Huai Mae Mhae watershed, Chiang Dao district, Chiang Mai Province.

2. Hydrometeorologic Charecteristic

Tipping bucket and data logger recording raingage were distributively installed over Huai Mae Mhae watershed. Locations, co-ordinates and elevations of all stations were tabulated in Table 12 and Figure 10.

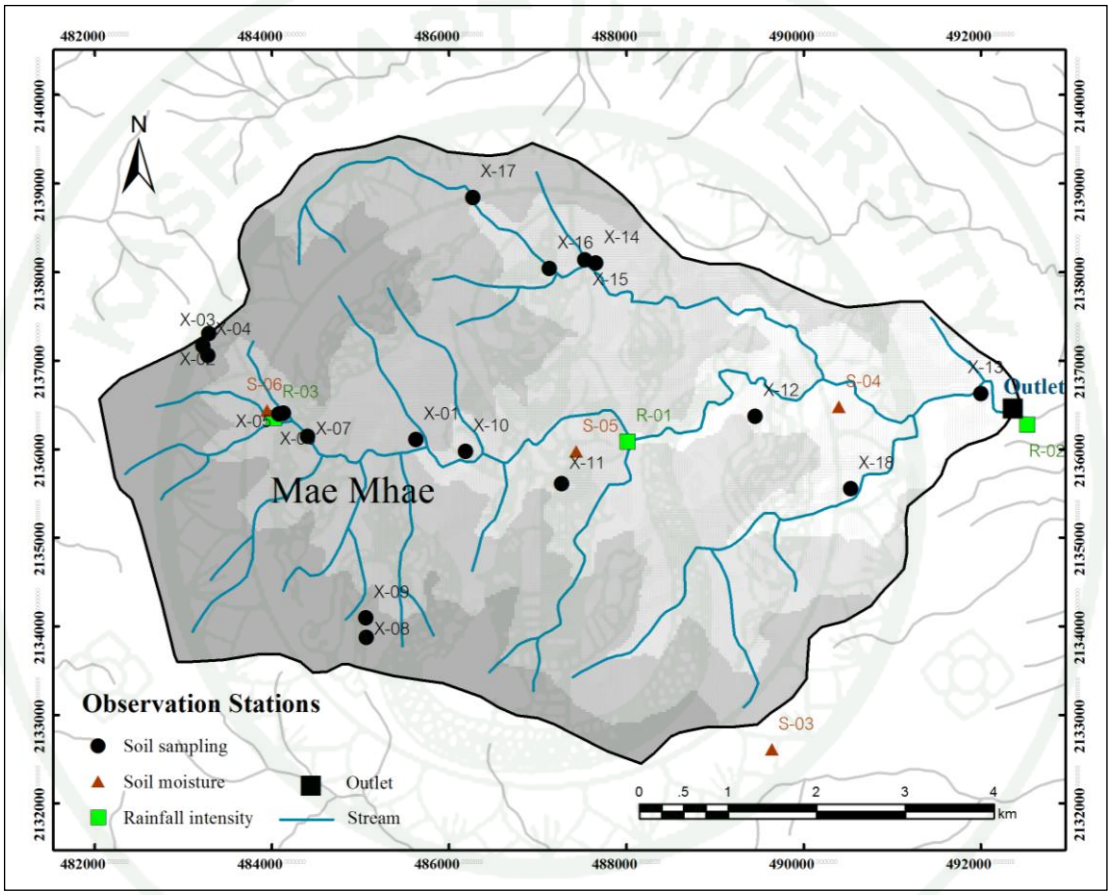

Figure 10 Tipping bucket and data logger recording rain gauge stations, soil sampling and soil moisture station at Huai Mae Mhae watershed.

Table 12 Co-ordinates of tipping bucket and data logger recording raingage stations at Huai Mae Mhae watershed.

Type	Station Name	N	E	Elevation (m)	Duration of data
Rain gauge	Outlet	2,136,272	492,526	479	25/5/53-3/11/53
Rain gauge	Ban Pang Mai	2,136,348	484,026	1136	17/6/53-3/11/53
Rain gauge	Ban Mae Na	2,137,300	495,413	377	25/5/53-3/11/53
Rain gauge	Ban Mae Mhae	2,136,080	488,015	753	22/8/53-28/10/53
Water level	Outlet	2,136,391	492,352	486	30/7/53-26/10/53
Water level	Ban Mae Na	2,137,303	495,419	377	20/9/53-28/10/53

Rainfall amount were measured at Huai Sai Khaow in mixed deciduous forest and Huai Mae Sai in evergreen hill forest between 2004 to 2010. Mean annual rainfall amount at Huai Sai Khaow and Huai Mae Sai during 2004 to 2010 are 1,583.1 and 2,105.9 mm respectively. Rainfall distribution in terms of isohyetal map of the Mae Mhae watershed during May to November 2010 were calculated and revealed that rainfall amount increase directly with increasing of elevation as shown in Figure 11. Mean annual rainfall were classified in percentage of mean annual rainfall amount for 5 subseasons (Silverman *et al.*, 1986) according to each type of monsoon. Percentage of rainfall during rainy season or Southwest Monsoon season (SM) at Huai Sai Khaow and Huai Mae Sai were 49.1% and 51.5% respectively as shown in Table 13 and Figure 12.

Spatial rainfall distribution in the high mountain at Mae Mhae watershed were directly increased with increasing elevation that contemporaneous with the results of many researchers such as amount of rainfall distribution on high mountain at Tha Wang Pha district, Thung Chang district and Ban Kok, Chiang Klang district, Nan province in northern Thailand were gradually increased with the increasing of elevation as 1,413 mm, 1,784 mm and 2,193 mm respectively (Udomchoke *et al.*, 2010).

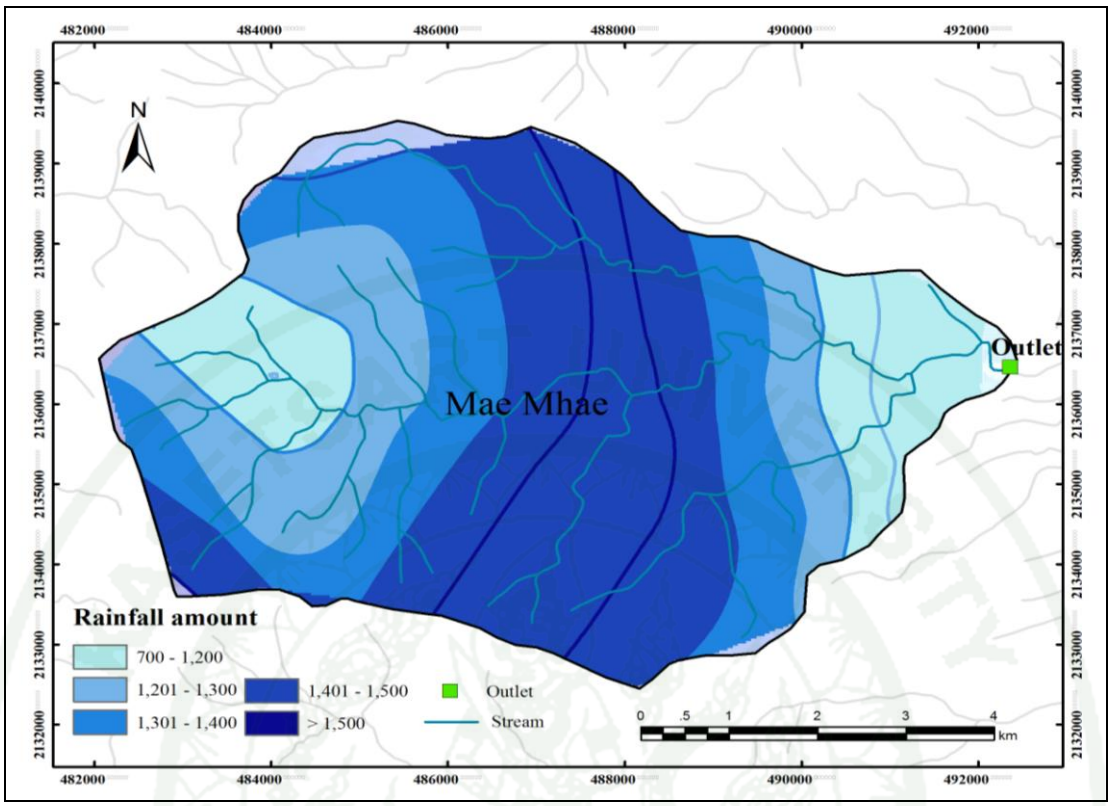

Figure 11 Isohyetal map of rainfall at Huai Mae Mhae watershed during May to November 2010.

Table 13 Mean annual rainfall percentage in each subseason of Huai Sai Khaow and Huai Mae Sai watershed (annually 1,583.1 and 2,105.9 mm) during 2004 to 2010.

Type of Monsoon	Duration	Percentage of annual rainfall (%)	
		Huai Sai Khaow	Huai Mae Sai
Northeast Monsoon Season (NM)	Nov - Feb	7.8	7.5
Summer Intermoonsoon Season (SIM)	Mar - Apr	7.0	7.3
Onset Southwest Monsoon Season (OSM)	May - Jun	26.9	25.7
Southwest Monsoon Season (SM)	Jul - Sep	49.1	51.5
Winter Intermonsoon Season (WIM)	Oct	9.2	8.0

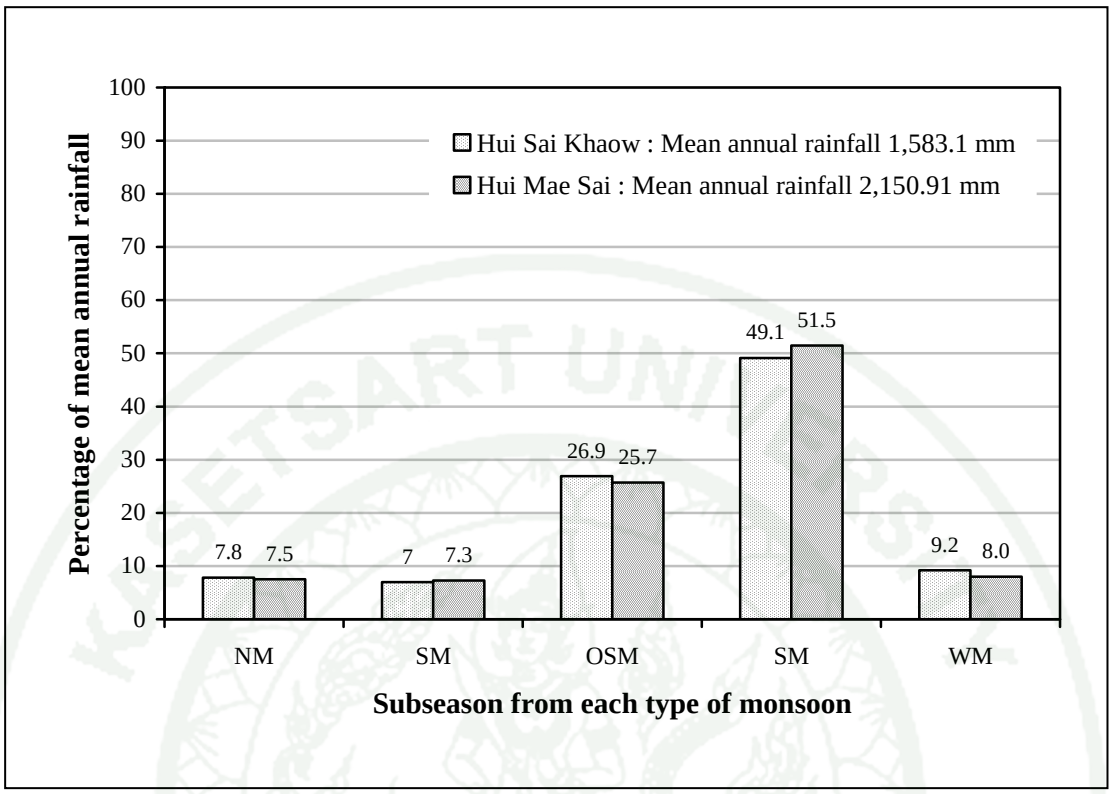

Figure 12 The percentage of average annual rainfall in each season from 2004 to 2010 at Huai Sai Khaow and Huai Mae Sai.

The temporal distributions of daily rainfall amount at Huai Sai Khaow and Huai Mae Sai for each subseason were analyzed. The result showed that mostly rainy days in each subseason range from 0.1 to 10.0 mm. During onset of the rainy season (OSM) and in the rainy season (SM), the rainy days of slightly heavy rain (60.1 – 90 mm) and heavy rain (> 90 mm) were two days and one day both in Huai Mae Sai and Huai Sai Khaow station as shown in Table 14 and 15 and Figure 13.

This temporal distribution implied that only one day chance of heavy rain occurred at Mae Mhae watershed that can cause landslide area on the hillslope as well as landslide risk area and flood on the undulating area and alluvium. Only one day or two day that heavy rain occurred on the high mountain watershed in Nan Province, northern Thailand.

Table 14 Number of rainy days of each rainfall amount and each subseason at Huai Sai Khaow watershed.

Season	no rain	Rainfall (mm) at Huai Sai Khaow station (Mixed Deciduous forest)							
		< 0.1	0.1-1.0	1.1-10.0	10.1-20.0	20.1-35.0	35.1-60.0	60.1-90	> 90
NM	58	0	55	3	2	1	1	0	0
SIM	46	0	5	6	2	1	1	0	0
OSM	12	0	13	22	7	5	2	0	0
SM	19	0	17	30	15	6	3	1	1
WIM	13	0	7	5	4	1	0	1	0
Total	148	0	97	66	30	14	7	2	1

Table 15 Number of rainy days of each rainfall amount and each subseason at Huai Mae Sai watershed.

Season	no rain	Rainfall (mm) at Huai Mae Sai station (Mixed Deciduous forest)							
		< 0.1	0.1-1.0	1.1-10.0	10.1-20.0	20.1-35.0	35.1-60.0	60.1-90	> 90
NM	94	0	19	4	2	1	0	0	0
SIM	45	0	6	6	2	1	1	0	0
OSM	9	0	12	22	8	5	4	1	0
SM	15	0	16	30	11	11	7	1	1
WIM	12	0	10	3	3	2	1	0	0
Total	175	0	63	65	26	20	13	2	1

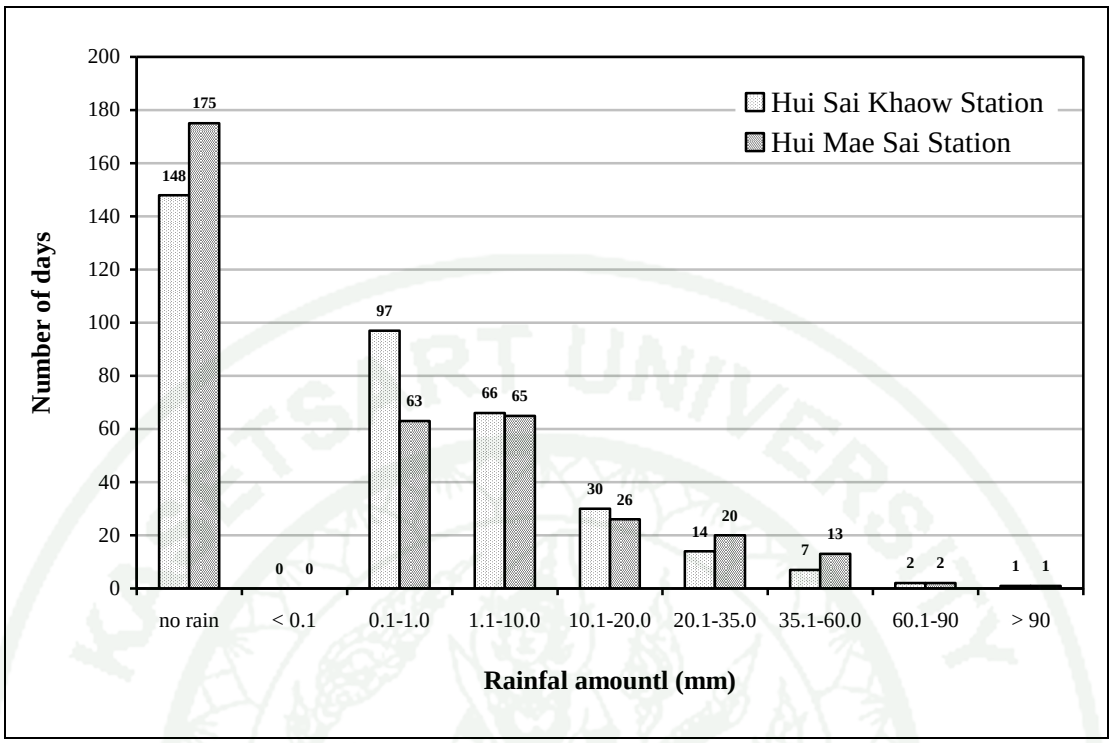

Figure 13 Number of rainy days of each rainfall amount of Huai Sai Khaow and Huai Mae Sai watershed.

The temporal distribution of annual rainfall amount were defined in wet year (high rainfall amount), normal year (normal rainfall amount) and dry year (low rainfall amount) from data of annual at meteorological station of Chiangdao district where located nearby the study area and is recorded since 1989 to 2009. Three groups of temporal annual rainfall distribution were tabulated in Table 16.

Table 16 Three groups of rainy years, wet normal and dry at Chiang Dao district meteorological station, 15 km from Mae Mhae watershed.

Rainy Year	Years
Wet	1994, 1995, 2001, 2003, 2005 and 2006
Normal	1989, 1993, 1997, 1999, 2000, 2002, 2007, 2008 and 2009
Dry	1990, 1991, 1992, 1996 and 1998

3. Landuse

Landuse of Huai Mae Mhae watershed were classified, identified and encroached from Satellite Image by Google Earth 2010 for hill evergreen forest, mixed deciduous forest, dry dipterocarp forest, tea plantation, orchard and corn. Boundary of each landuse type in satellite image were digitized by Google Earth software, then field survey for boundary verification were carried out as shown in Figure 14. Tea plantation always exists on the ridge top to north aspect due to south aspect as related to Figure 8. Land utilization map of Mae Mhae watershed were classified as hill evergreen forest and tea and orchard plantations as shown in Figure 15. From resolution of DEM 30 m × 30 m as encroached from Satellite by Google Earth 2010 showed quite difference between hill evergreen forest ares and orchard as well as tea plantation area. This advantage of geographical Information Technology in the present day can easily confirm landuse those were obtained from satellite images and the reality sites.

Figure 14 Identification of encroaching area by digitizing from Google Earth in 2010.

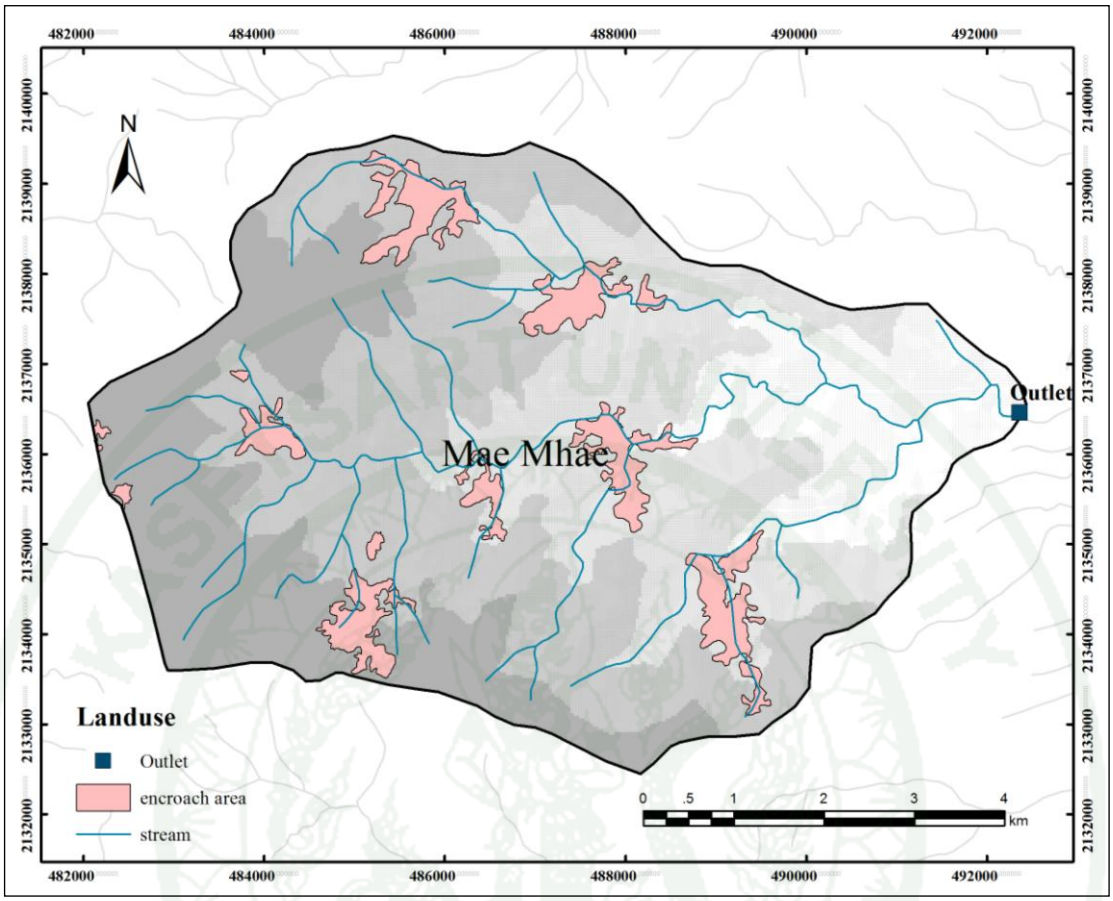

Figure 15 Land utilization map of Huai Mae Mhae watershed.

4. Geology

Geology of the study area is mainly granitic rocks regarding to plutonic intrusion during Triassic period. Minerals composition of granite in this area are mainly quartz (31.8%), plagioclase (28.9%) alkali feldspar (21.9%) and biotite (17.38%) were reported by Anonglak (1989). Biotite granite was found nearby ridge top or watershed boundary. Granite those mainly quartz and feldspar composition exist at lower elevation of watershed area. Granite those occurs in Southeast, South, Southwest and west aspect show rather shallow surface soil (< 0.5 to 1 m or more) and overlay on top of highly weathered granitic rock (weathering grade V) or coarse quartz grained sandy soil from 0.5 or 1 m to > 5 m. Granite those exists in East, Northeast, North and Northwest aspect always show deep top soil with clayey sandy

loam texture (1 m to 1.5 m or more) and overlay on top of highly weathered granitic rock or sandy soil from 1 m or 1.5 m to > 5 m depth. These soil sections were observed along road cut from footslope to ridge top of the mountain range in Huai Mae Mhae watershed as shown in Figure 16 and 17. Geologic map and soil sampling station are shown in Figure 18.

Major feature of quartz grained sandy soil or grade V weathered granite those derived from both biotite granite and quartz-feldspar granite are coarse quartz grain that easily breakdown to fine and very fine quartz grained sand. This quartz grain characteristic influence on internal friction angle of this non cohesion soil (weathered grade V granite) from high to low value, then stability of slope were also deceased.

Figure 16 Saprolite of granite (mainly quartz and feldspar) at depth 4 m from ground surface (top), close up texture of feldspar, quartz and biotite (bottom).

Figure 17 Saprolite of biotite granite (weathering grade V) at depth 5 m from ground surface (top) and close up texture of biotite, quartz and feldspar (bottom).

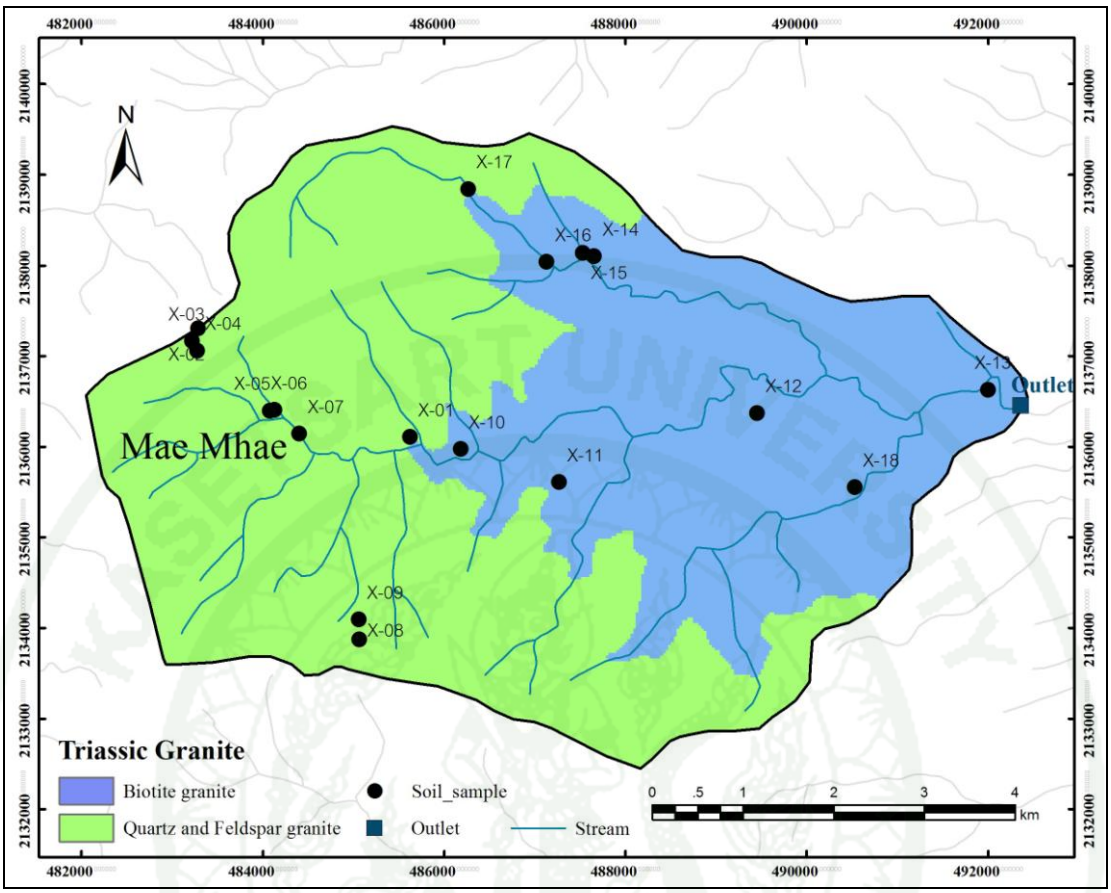

Figure 18 Map of biotite granite and quartz and feldspar granite in Triassic age and soil sampling locations at Huai Mae Mhae watershed.

5. Soil

Soil in the study area is mainly derived from granite that easily slides down from steep slope under the influence of higher saturation due to heavy rain. Eighteen locations along roadcut routes from outlet to ridge top of Huai Mae Mhae watershed were visited. Soil profile, depth, disturbed sampling and undisturbed sampling were carefully identified and taken. Northeast to Northwest aspect exists clayey sandy loam texture on the surface at the depth range between 0.5 to 1.5 m or more, deeper than surface soil are highly weathered granite with mainly coarse weathered feldspar and quartz minerals or coarse sandy soil. Soil in the Southeast and Southwest aspect showed clayey sandy loam texture only in the shallow surface soil (< 0.5 m). The sandy texture shows in the deeper zone of this aspect. The difference between soil

texture and soil depth of the North aspect and the South aspect cause by the location of study area is on latitude 18 to 19 degree North that solar radiation always shine on the South aspect than the North aspect, then North aspect will wetter than the South as well as higher weathering rate of rock to soil than the south and cause deeper surface soil.

Texture of each soil profile, slope, aspect and elevation of eighteen stations were tabulated in Appendix Table 1.

6. Antecedent Precipitation Index (API)

A. Antecedent Precipitation Index from Recession Flow

Recession coefficient (K_r) of the watershed was analyzed from stream flow data. Three steps in one row rectangular weir and automatic water level recording by data logger were constructed at the outlet of Mae Mhae channel. Recession coefficient of Huai Mae Mhae watershed of each hydrograph ranged between 0.96 to 0.99. Initial API was obtained from dry condition (in March) or nearly permanent wilting moisture content of deep soil to surface soil as shown in appendix Table 2. Consecutive rainfall of previous year were applied to calculated API based on concept of Linsley *et al.* (1998) that accompanied with recession coefficient of moisture content in soil that slowly drain from deep soil to channel as shown in equation (4). Transient values of API that obtain from consecutive rainfall at three representative stations (Ban Mae Sai, Ban Mae Mhae and Ban Pang Mai) of Mae Mhae watershed were plotted in Figure 19.

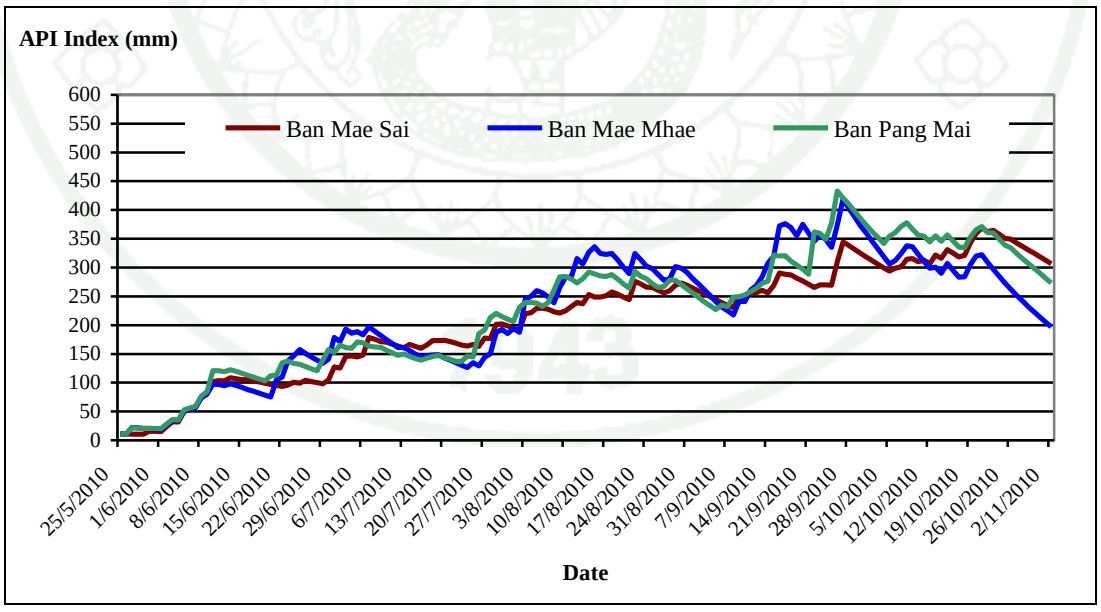

Figure 19 Antecedent Precipitation Index (API) of Mae Mhae watershed (by Recession flow method) at Ban Mae Sai, Ban Mae Mhae and Ban Pang Mai.

After consecutive rainfall were calculated through recession coefficient, the maximum API yielded about 370, 425 and 440 mm for station at Ban Mae Sai, station at Ban Mae Mhae and station at Ban Pang Mai respectively. In case one day, two days and three days continually rainfall with 100 mm per day, the calculated maximum API at Ban Mae Sai, Ban Mae Mhae and Ban Pang Mai were 492, 429 and 508 mm for one day 100 mm rainfall, 575, 529 and 592 mm for 2 days 100 mm consecutive rainfall and 654, 618 and 675 mm for 3 days 100 mm consecutive rainfall respectively.

B. Antecedent Precipitation Index from Curve Number

Curve Number of Mae Mhae watershed for API calculation were carried out following concept of Ornarsa *et al.* (2010) as shown in appendix Table 3 and 4. The consecutive rainfall from May, 5th to October 21st, 2010 were applied to calculate API by Curve number concept and obtained three curves of API for three locations in Mae Mhae watershed as shown in Figure 20, 21 and 22. Maximum API from this method at Ban Mae Sai, Ban Mae Mhae and Ban Pang Mai at depth 100 to 200 cm were 180, 157 and 174 mm respectively. Combine API of all depth from surface to more than 200 cm obtained maximum API through section of soil (~200 cm) at Ban Mae Sai, Ban Mae Mhae and Ban Pang Mai were 345, 370 and 340 mm respectively.

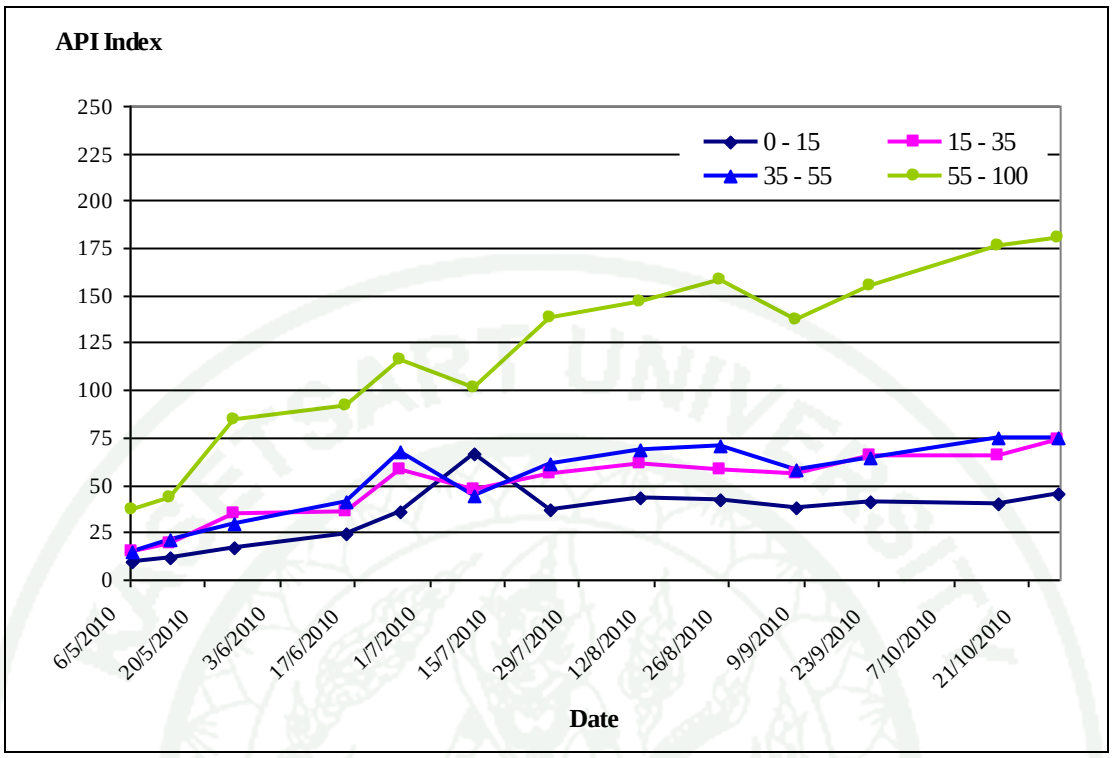

Figure 20 API index of Ban Mae Sai from May 5th 2010 to October 21st 2010.

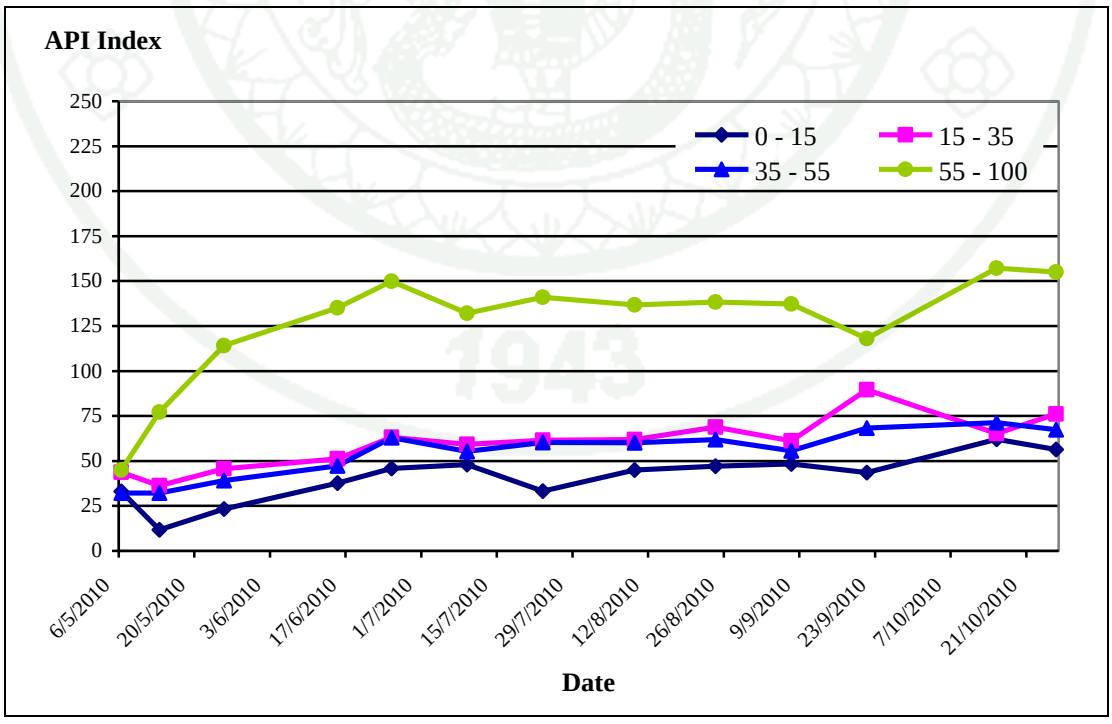

Figure 21 API index of Ban Mae Mhae from May 5th 2010 to October 21st 2010.

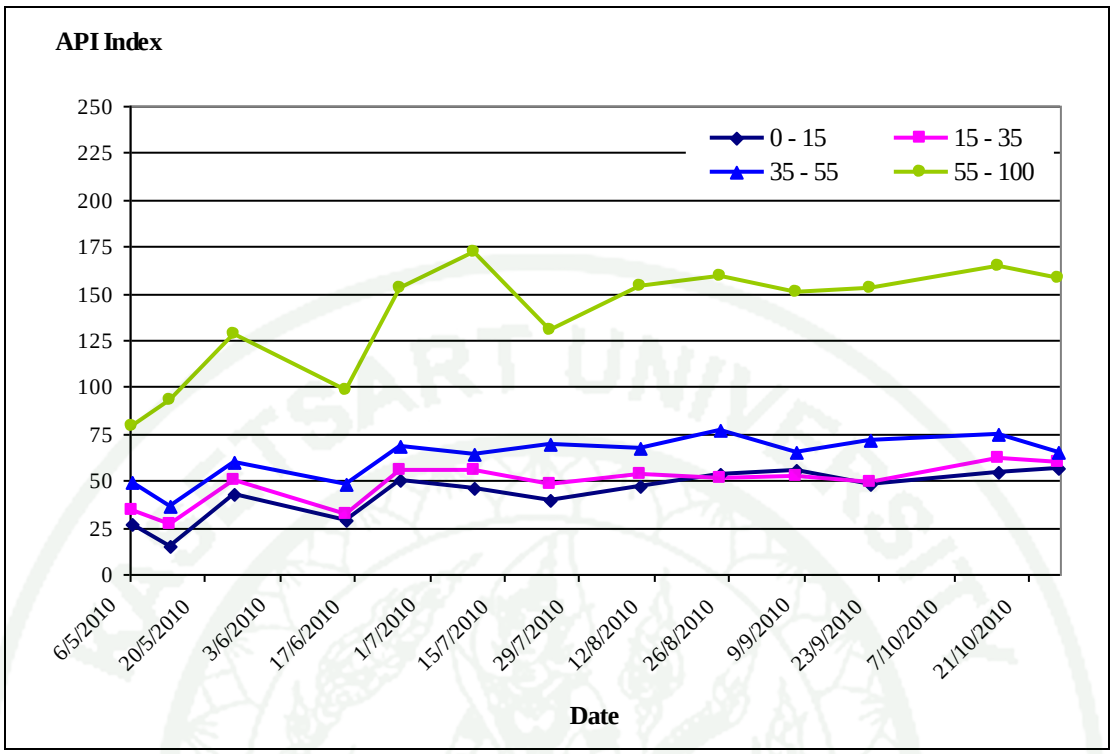

Figure 22 API index of Ban Pang Mai from May 5th 2010 to October 21st 2010.

C. Antecedent Precipitation Index from Weather Reaserch and Forecasting (WRF) Model

Infiltration rate of soil after raining were calculated from Richard's equation in WRF model for the API calculation Module as shown in appendix table 5. Spatial distribution of daily rainfall were predicted by WRF model from radiosonde data or upper atmospheric acqussition data of multilayer climatic factors module. Calculated API by WRF model at three locations in Mae Mhae watershed were obtained in Figure 23, 24 and 25. Maximum API calculated from WRF model of these locations at depth between 100 to 200 cm at Ban Mae Sai, Ban Mae Mhae and Ban Pang Mai were 372, 368 and 378 mm respectively. The resolution of WRF grid (4 km × 4 km) may too large to use with small watershed, but in case of predicted rainfall model, the calculated API from upper atmospheric condition are reasonable.

Comparison of critical API value from three methods showed that critical API value from recession flow method are very good fit with critical API value from WRF model. Critical API from the calculation of total soil porosity and effective depth revealed the contemporaneous results with critical API from WRF and recession flow method.

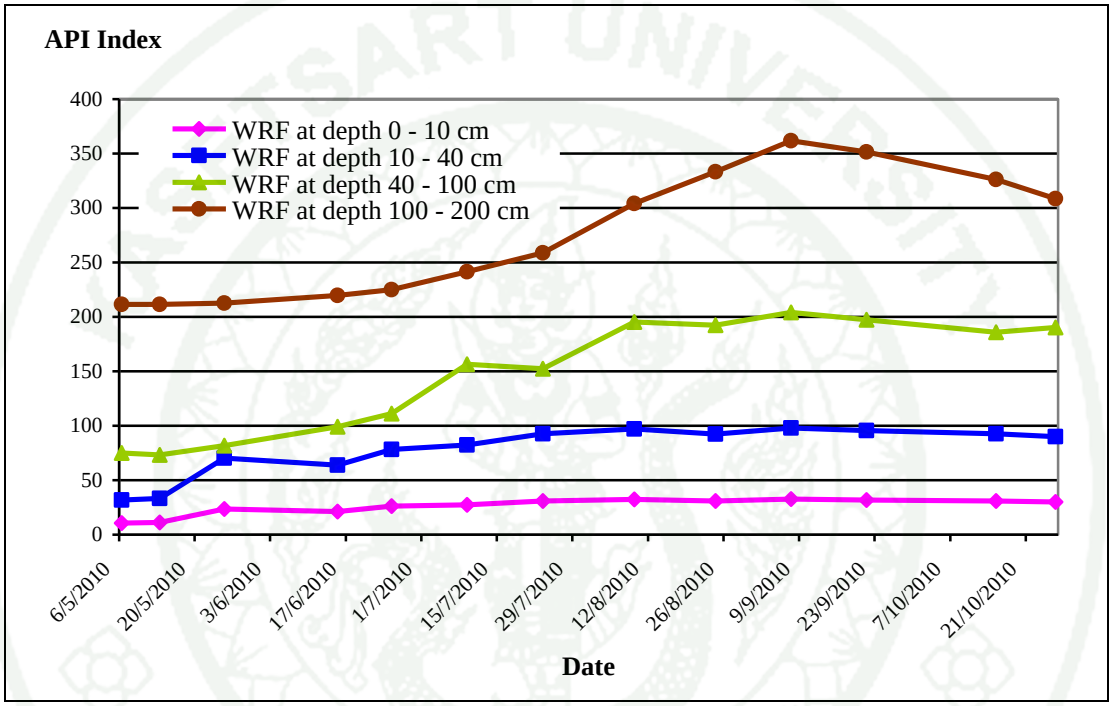

Figure 23 Antecedent Precipitation Index (API) at Ban Mae Sai of Mae Mhae watershed by WRF model.

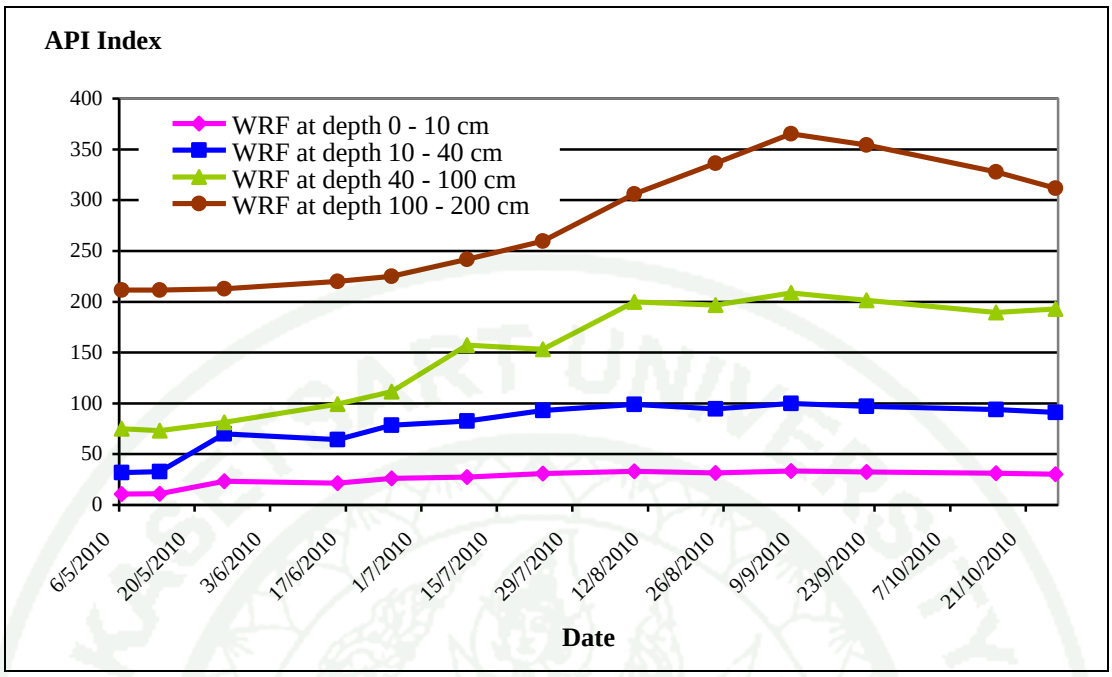

Figure 24 Antecedent Precipitation Index (API) at Ban Mae Mhae of Mae Mhae watershed by WRF model.

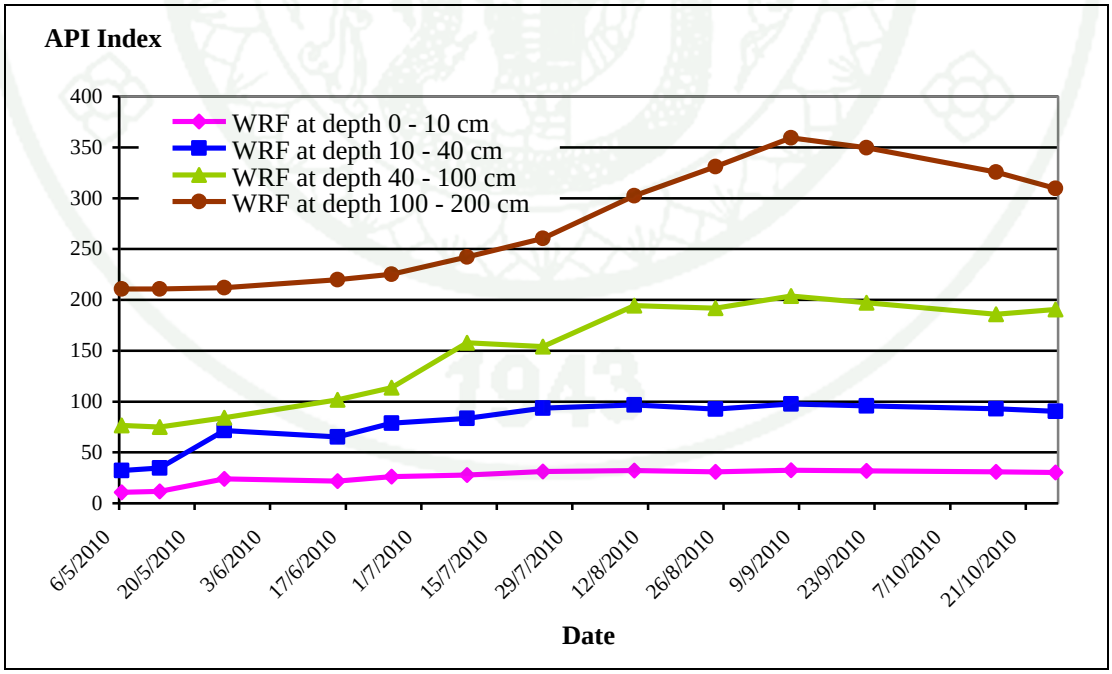

Figure 25 Antecedent Precipitation Index (API) at Ban Pang Mai of Mae Mhae watershed by WRF model.

7. Slope Stability Analysis

A. Effective Depth

The effective depth or depth of weak plane that cannot support driving force or driving moment due to loss of shear strength after all soil pores nearly fulfill with water. The effective depth of the slope area can be roughly estimated from the boundary of soil profile between B profile to C profile. Texture of A and B profile of soil in this area those derived from Triassic granite are dominantly sandy clay loam, but sandy to sandy loam for C profile.

Eighteen locations along roadcut of three main router on the mountain were visited (Figure 10) their soil profiles as well as soil properties were also investigated. Depth soil profile, texture, aspect, slope elevation and disturbed as well as undisturbed sample were carried out as shown in Table 17. Relationships between depth of soil profile B-C and slope, aspect and elevation were calculated and conclude. Effective depth (Z in meters) decrease exponentially with azimuth angle (θ in degree) and correlation coefficient (R^2 is equal to 0.53) equation (5) and Figure 26.

$$Z = 5.9032 \exp(-0.0028\theta) \quad (5)$$

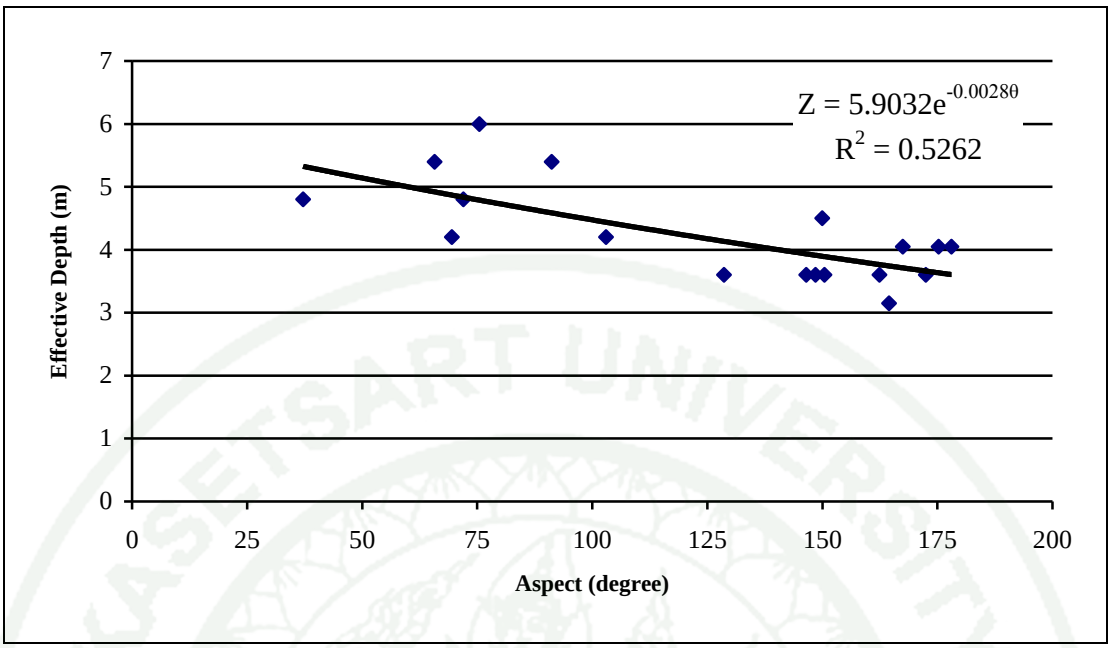

Figure 26 Relationship between effective depth (Z) and aspect in term of azimuth angle (θ) at Huai Mae Mhae watershed.

Effective depth (Z) for all elevations those vary with slope of watershed (β) are in function of exponentially decay as in equation (6) and (7) and as shown in Figure 27 and 28 for North aspect and South aspect respectively.

For North aspect (0 - 90° and 27° - 360°, $R^2 = 0.89$)

$$Z = 6.170 \exp(-0.006\beta) \quad (6)$$

For South aspect (91° - 270°, $R^2 = 0.64$)

$$Z = 4.561 \exp(-0.008\beta) \quad (7)$$

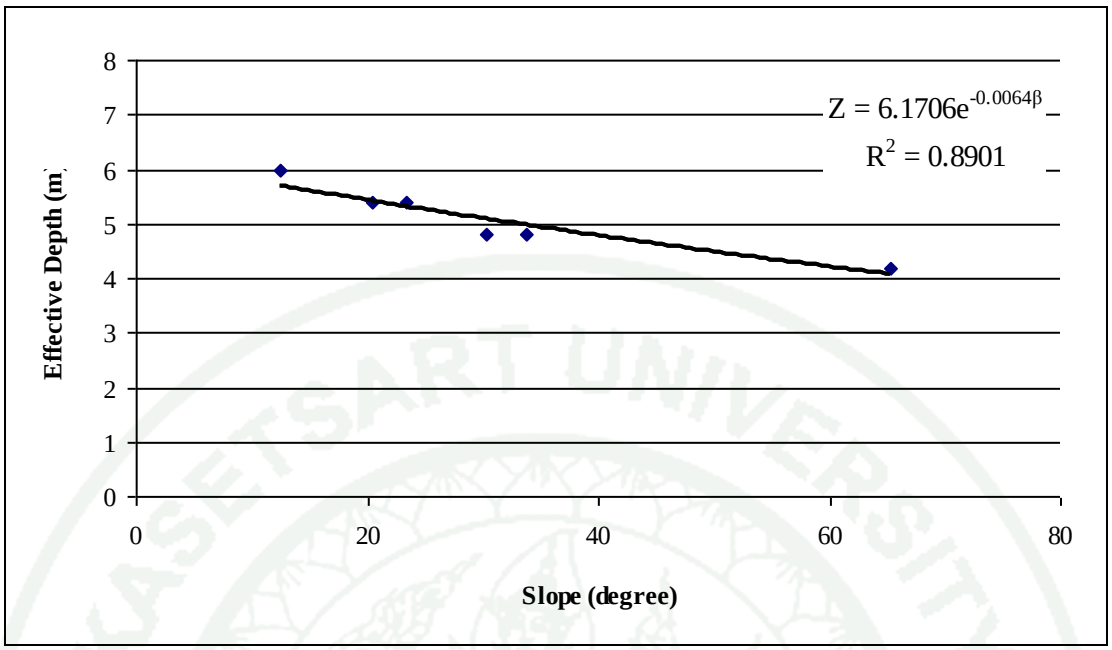

Figure 27 Relationship between effective depth (Z) and slope of the watershed (β) in North aspect at Huai Mae Mhae watershed.

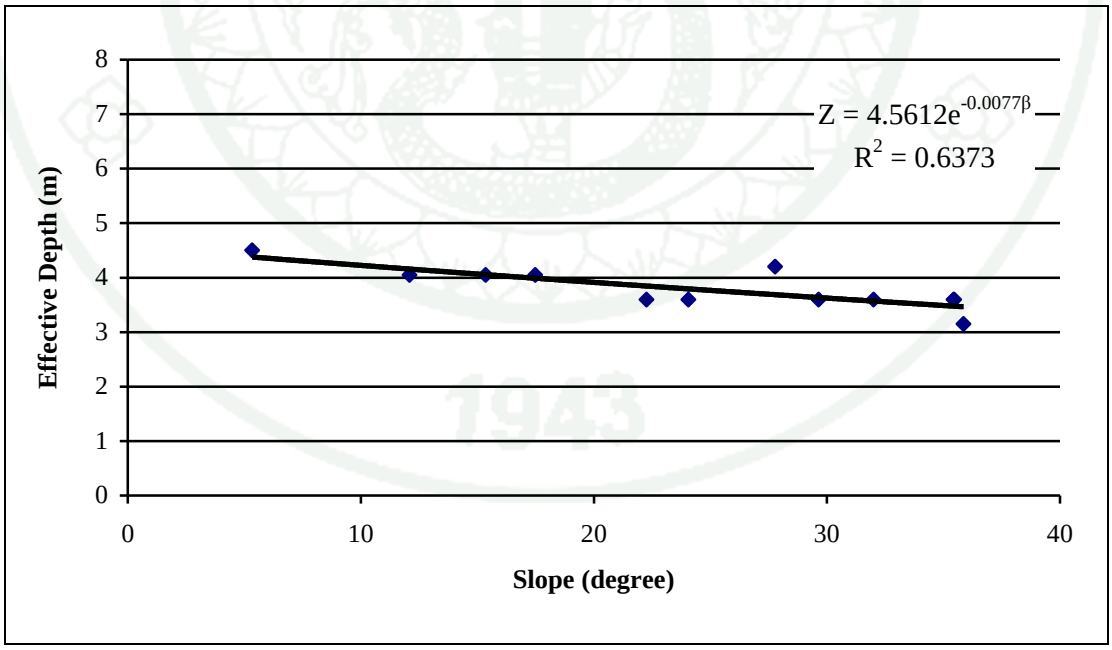

Figure 28 Relationship between effective depth (Z) and slope of the watershed (β) in South aspect at Huai Mae Mhae watershed.

In case of relationships between effective depth and elevation, there are three conditions those were calculated as follows:

For gentle to slightly steep slope (0 - 17 degree, $R^2 = 0.75$) the effective depth increase exponentially with elevation (h in meters) for all aspect as in equation (8) and Figure 29.

$$Z = 1.0749 \exp(-0.0012\beta) \quad (8)$$

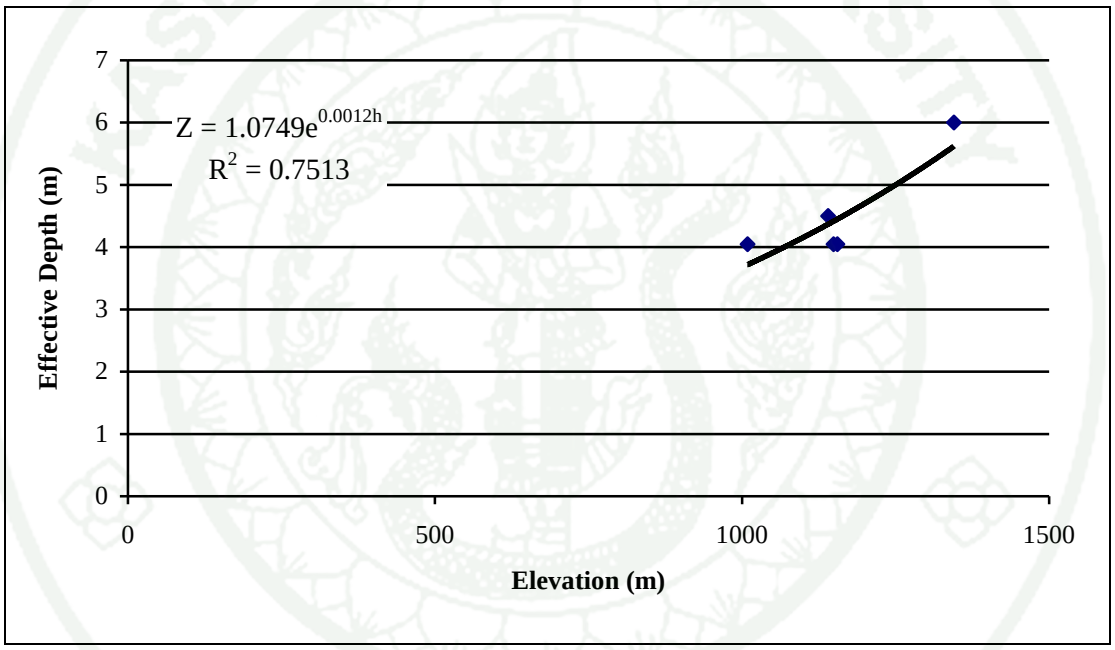

Figure 29 Relationship between effective depth (Z) and elevation (h) of Mae Mhae watershed in case of gentle slope 0 – 17 degree.

For higher slope than 17 degree, the effective depth vary with elevation as gradually decrease exponentially both in North aspect and South aspect and Figure 30 and 31 respectively.

For N aspect (slope > 17°, $R^2 = 0.47$)

$$Z = 5.9479 \exp(-0.0002h) \quad (9)$$

For S aspect (slope > 17°, $R^2 = 0.41$)

$$Z = 4.2922 \exp(-0.0002h) \quad (10)$$

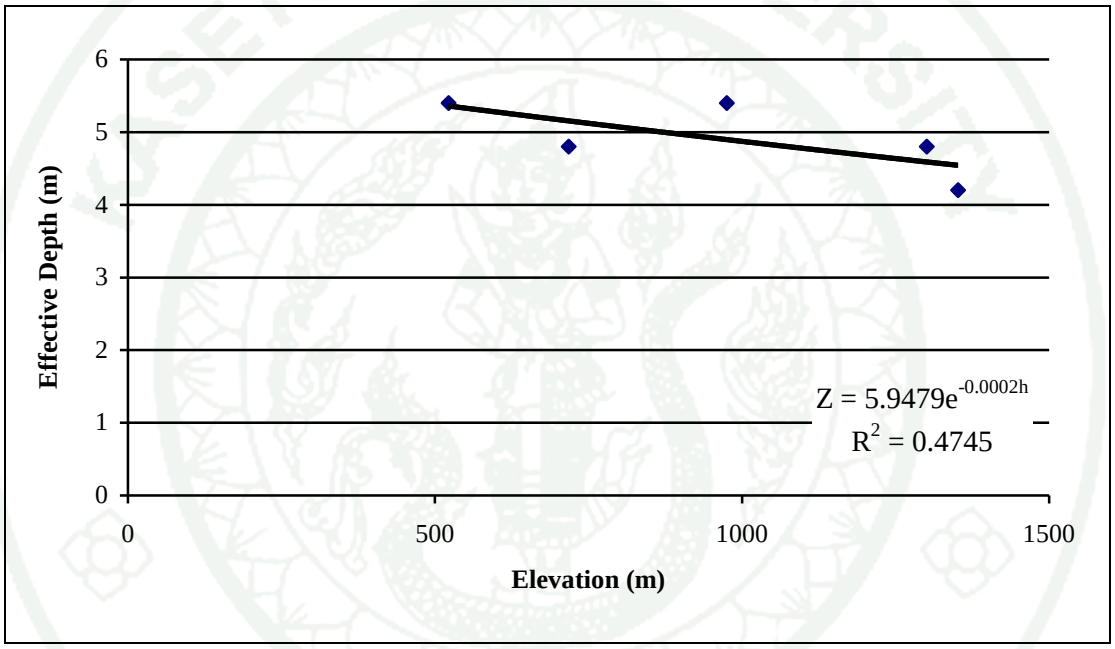

Figure 30 Relationship between effective depth (Z) and elevation (h) of Huai Mae Mhae watershed in case of steep slope and Northing orientation.

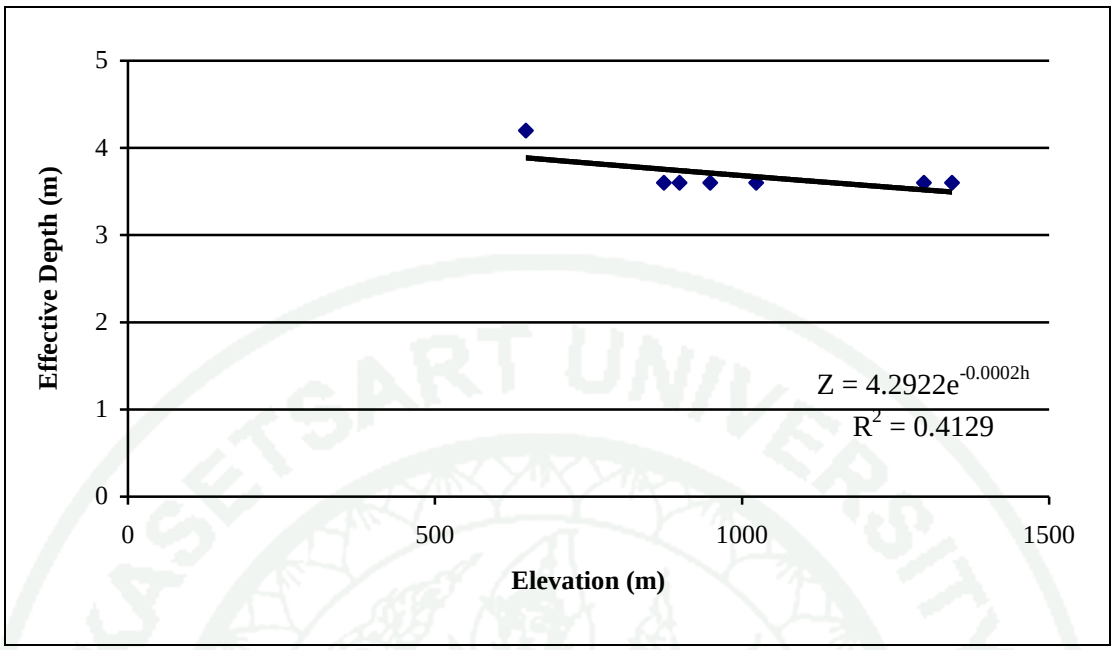

Figure 31 Relationship between effective depth (Z) and elevation (h) of Huai Mae Mhae watershed in case of steep slope and Southing orientation.

Input, slope, aspect and elevation for each grid (30 m x 30 m), then calculate effective depth of the watershed those response to stability of slope to fail down at nearly saturated moisture content as shown in Figure 32.

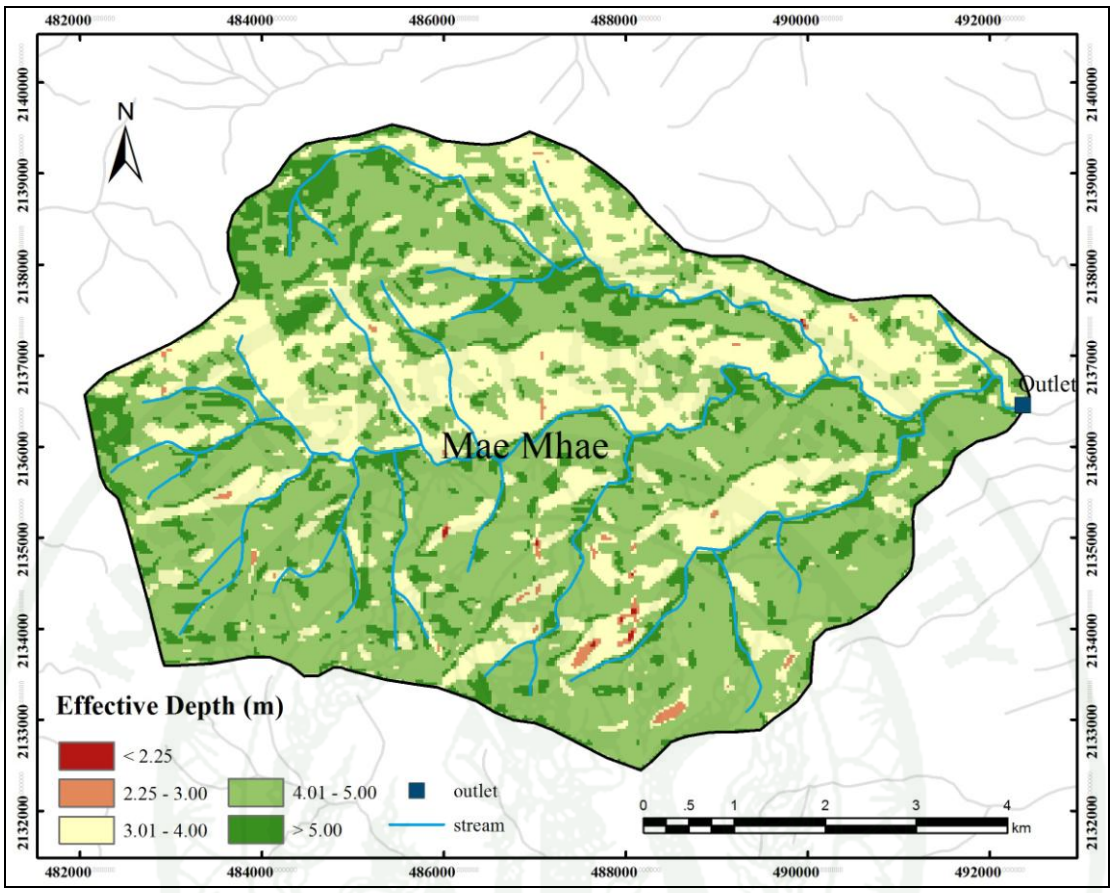

Figure 32 Numerical grid calculation of effective depth in Huai Mae Mhae watershed**.**

Calculated value of effective depth those obtained from profile along roadcut of three major routes in the watershed were compared with the effective depth in granitic area those yielded from those geostatistically predicted by Penizek and Boruvka (2006). Result of the comparison are quite agree together that the effective depth depend on aspect, slope and elevation.

B. Soil Strength

Direct shear test were carried out at Ban Mae Sai (2,135,214N and 491,049E) and Ban Mae Mhae (2,135,852N and 488,474E) on residual soil derived from granite and biotite granite respectively. Cohesion and inter friction angle of granite soil and residual soil from biotite granite are 2.52 and 2.73 kPa and 10.2 and

8.4 degree respectively. These soils were shear at almost saturation condition on C profile (weathering grade V). Testing data were tabulated in Appendix Table 6 to 7 and Appendix Figure 5 to 8. Soil cohesion value of C profile are quite low when compare with sandy clay loam soil of the A and B profile due to the incomplete weathering of feldspar in granite to clay composition of soil in C profile. The internal friction angle in C profile are quite low when compare with sandy soil those derived from granite at another locations (Appendix Table 8) may due to the over stress condition that used to act at this quartz grained sand. After weathering activities on the large porphyritic quartz grain from fresh rock to slightly completely weathered rock, the large quartz grain become fine sand and vary fine sand size and cause the low value of internal friction angle.

C. Land slide risk map

Cohesion of soil reinforced by roots of hill evergreen trees was estimated from reports of many researchers as shown in Appendix Table 9 (Schmidt, 2001). Due to lack of these data for hill evergreen forest, the minimum value of soil cohesion reinforced by small roots and surcharge pressure of hill evergreen forest overlain on the surface soil were 30 kPa and 10 kPa respectively cohesion of soil reinforced by roots of tree plantation and orchards were estimated as 3 kPa due to very rare roots penetrate down from B profile to C profile.

Landslide risk map was created from the results of calculated slope stability factor of each grid. The minimum resolution of grid is 30 m x 30 m and layer by layer overlain together. Soil moisture content was assigned at critical API moisture content in order to perform high reliability landslide map.

At critical API moisture content, soil profile becomes nearly saturated throughout the section. Section along road cut shows very deep soil profile. The results revealed that there are 5 level of area those subjected to landslide as shown in Table 17 and Figure 33. Detail of landslides are:-

1. Area of very highly land slide risk about 0.21 km^2 or 0.45% of total watershed area located on tea plantation and orchard with safety factor of slope stability between 0 to 0.5.

2. Area of highly land slide risk about 1.94 km^2 or 4.20% of total watershed area located on tea plantation and orchard with safety factor of slope stability between 0.5 to 1.0.

3. Area of moderately land slide risk about 1.20 km^2 or 2.59% of total watershed area that located on dry dipterrocarp forest, steep slope and oriented in Southeast, South and Southwest aspect with safety factor of slope stability range between 1.0 to 1.25.

4. Area of low slide risk about 4.29 km^2 or 9.25% of total watershed area that located on hill and rolling area with safety factor of slope stability range between 1.25 to 1.5.

5. Area of no land slide risk about 38.7 km^2 or 83.51% of total watershed area that located on undulating area with safety factor of slope stability greater than 1.5.

The area of high risk of land to slide down from sloping landform was subjected to the opened forest area to tea plantation and orchard. In case of gentle slope of this landuse such as on ridge top, this landuse existed low risk of land to slide that quite reasonable to existing condition whereas at gentle slope near by the creek show high risk of landslide due to their higher saturation condition in soil that initially subjected to landuse.

Table 17 Areal distribution of landslide risk in Huai Mae Mhae watershed.

FS	0 – 0.5	0.5 - 1.0	1.0 – 1.25	1.25 – 1.5	> 1.5
Area (km^2)	0.21	1.94	1.20	4.29	38.70
Area (%)	0.45	4.20	2.59	9.25	83.51

The application of Numerical Grid model to determine the landslide risk map based on the deterministic concept that difference from the landslide risk factor (LRF) method those used to use by Udomchoke and Chokesomboonkul (1999) that can be properly used with each proper location those used to face with landslide in the past. This method are quite difference from the lump deterministic model that followed by Solalump amd Chotikasathien (2007) that used weighting factor in landslide risk mapping. Numerical grid method show more advantage than other method due to the real data input in terms of grid to grid.

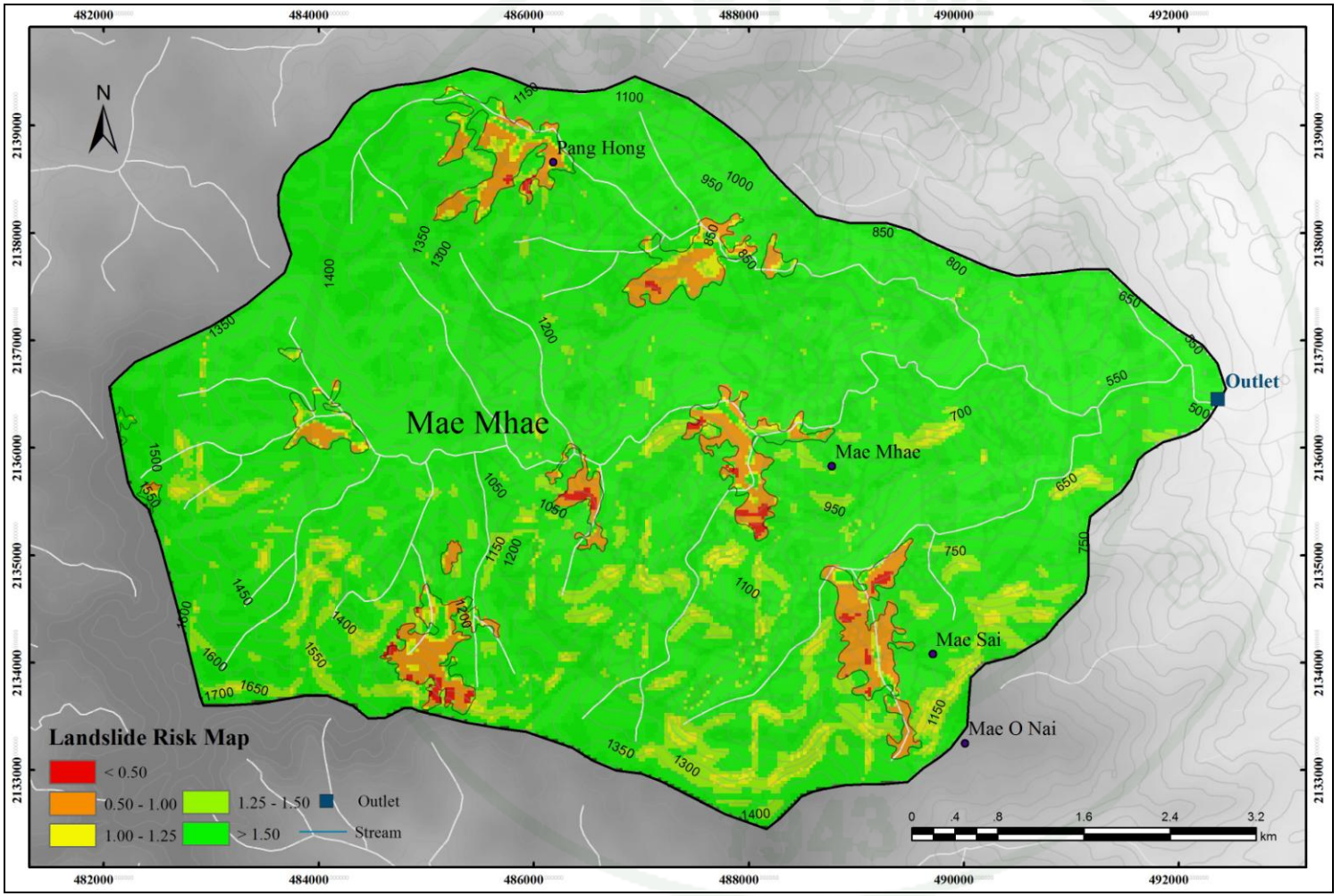

Figure 33 Landslide risk map created from slope stability analysis by numerical grid model.

CONCLUSION AND RECOMMENDATION

Conclusion

1. Critical API values those obtained from recession flow are quite agreed with critical API value from WRF method and critical API from soil porosity and effective soil depth. Critical API subject to landslide ranged between 340 to 370 mm.

2. Effective depth of landslide area is under the influence of aspect, elevation, and slope of the watershed. Soil depth of each grid was exponentially decreased with aspect from North to South and with slope as well as elevation. Aspect is the major influence on effective depth of very steep slope soil in term of exponentially change with elevation. Soil depth in the North aspect at the elevation higher than 1000 m in hill evergreen forest were found deeper than 5 m. Soil depth in the South aspect at the same elevation and same landuse are lesser deep.

3. Numerical square grid model of 30 m × 30 m were used to calculate slope stability factor of the watershed area resolution. Open source GIS named Map Server were use as tool for calculation and presentation. The translational infinite slope were applied to create landslide map.

4. Map of landslide area was created for Mae Mhae watershed those are compered area of very highly landslide, highly landslide, slightly high landslide, low landslide and no landslide are 0.21, 1.94, 1.20, 4.29, and 38.70 km^2 or 0.45%, 4.20%, 2.59%, 9.25% and 83.51% respectively.

5. Very high landslide areas were mapped in the steep slope zone, tea plantation and orchard, south aspect and in the biotite granitic rock.

Recommendation

The recommendations of this study are as follows:

1. Rotation slide concept should be applied in the future research as well as surcharge load from hill-evergreen forest should be more study in detail.

2. Effective depth of the watershed area those subjected to landslide should be more sites visited and calculated by another method, then confirmed them together more precise equation.

3. Strength of soil under the influence of roots of large tree and small tree in many types of forest and many type of tree should be carried out.

4. Small size of grid in WRF model for precision rainfall intensity from cloud by the accompany between cloud satellite data and radiosonde data those input into the WRF model should be carried out in order to obtain more precise rainfall intensity in each grid cell.

LITERATURE CITED

Anbalagan, R. 1992. **Terrain Evaluation and Landslide Hazard Zonation for Environmental Regeneration and Land Use Planning in Mountainous Terrain.** Christ church, Newzeland.

Anongrak, N. 1989. **The Genesis of Highland Soils Derived from Granitic Rocks in the Upper North of Thailand.** M.S. Thesis, Chiang Mai University.

Bishop, A.W. 1955. The use of the slip circle in the stability analysis of slopes. **Geotechnique** 5 (1): 7-17.

Braja, M. D. 1979. **Introduction to soil mechanics.** The Iowa State university Press, Iowa, USA.

Bunopas, S. and, P. Vella. 1978. Late Paleozoic and Mesozoic structural evolution of northern Thailand; a plate tectonics model, pp. 133-140. *In* **Proceedings of the Third Regional Conferences on Geology and Mineral Resources of Southeast Asia**. 14-18 November 1978, Asian Institute of Technology. Bangkok.

Chokesomboonkul, P. and V. Udomchoke. 1999. Risk Area Classification for Natural Hazards in Pak Phanang Watershed, Nakhon Si Thammarat Province, pp. 360 - 367. *In* **Proceedings of Kasetsart University Annual Conferences** 37th, 2 - 4 February 1999, Bangkok.

Chow, V. T, D. R. Maidment and L. W. Mays. 1988. **Applied Hydrology.** McGraw-Hill, New York, USA.

Coates, D.R. 1977. Landslide Perspective. **The Geological Society of American** 3: 3-28.

Cruden, D.M. 1991. A Simple Definition of a Landslide. **Bulletin of the International Association of Engineering Geology** 43: 27-29.

Cruden, D.M. and D. J Varnes. 1996. Landslide types and processes, pp. 36–75. *In*: Turner A.K.; Shuster R.L. (eds). **Landslides: Investigation and Mitigation. Transp Res Board**, Spec Rep 247.

Department of Water Resources. 2005. **Final Report on Landslide and Flood Risk Area of Thailand**; AnnexV (Appendix) on soil strength parameters of mountainous soils derived from specific rock unit in Thailand.

Fellenius W. 1927. **Erdstatische Berechnungen mit Reibung und Kohäsion (Adhäsion) und unter Annahme kreiszylindrischer Gleitflächen**. Ernst & Sohn, Berlin.

Hamblin W. Kenneth and H. Eric Christiansen. 2003. **Earth's dynamic systems**. 10th ed. Prentice Hall, USA.

Hammond C., D. Hall, S. Miller and P. Swetik. 1992. **Level I Stability Analysis (LISA) Documentation for Version 2.0**. General Technical Report INT-285, USDA Forest Service, Intermountain Research Station, Department of Agriculture, Ogden, Utha, USA.

Hunt, R.E. 1984. **Geotechnical Engineering in investigation manual.** McGrew-Hill, USA.

Inthacha, S., J. Kreasuwun and W. Promnopas. 2004. Numerical Weather Simulation of the Chanthu depression track by WRF**.** *In* **30th Congress on Science and Technology of Thailand**, 19-21 October 2004, Bangkok.

Jotisankasa, A. and A. Sawangsuriya. 2008. Application of unsaturated soil mechanics for slope stability. *In* **National Civil Engineering Conference 13th. Thailand.** 14-16 May 2008, Pattaya, Thailand.

Keller, H.B. 1968. Numerical Methods for two – points Boundary Value Problems, pp. 7–18; 39–71. *In* **A Blaisdell book in numerical analysis and computer science**, Blaisdell, Waltham, MA.

Schmidt, K.M., J.J. Roering, J.D. Stock, W.E. Dietrich, D.R. Montgomery and T. Schaub. 2001. The variability of root cohesion as an influence on shallow landslide susceptibility in the Oregon Coast Range. **Can. Geotech** 38: 995 - 1024

Lehmann,T. and H Holzmann. 2008. Flood warning level forecasting for ungauged catchments by Means of a combined API storage concept. *In* **XXIVth Conference of the Danubian Countries;.Series: Earth and Environmental Science 4**. IOP Publishing, Austria.

Linsley, R., Kohler, M., and Paulhus, J. 1988. **Hydrology for engineers**. McGrew-Hill, Inc. USA.

Lynn, B. and Y. Yair. 2010. Prediction of lightning flash density with the WRF model. **Advance in Geosciences** 23: 11-16.

Montgomery, D. R. and W. E. Dietrich. 1994. A Physically Based Model for the Topographic Control on Shallow Landsliding. **Water Resources Research**, 30(4): 1153-1171.

Organization of American States. 1991. **Primer on natural hazard management in integrated regional development planning.** Department of Regional Development and Environment. Washington, D.C., USA.

Ornarsa, S., P. Witthawatchutikul, A. Bonsanener, P. Triphattanasuwan, P. Bunsophit, C. Ornarsa and S. Siripaipan. 2010. **Modeling for Flood Warning on mountainous watershed at Namkhor Watershed**. National Park, Wildlife and Plant Conservation Department.

Pack, R.T., D.G. Tarboton, C.N. Goodwin and A. Prasad. 2005. **Sinmap User's Manual (A Stability Index Approach to Terrain Stability Hazard Mapping, technical description and users guide for version 2.00).** Utah State University, USA.

Penizek, V. and L. Boruvka. 2006. Soil depth prediction supported by primary terrain attributes: a comparison of methods**. Plant Soil Environ** 52: 424 – 430.

Phisit, D.,T. Wongwanich, W. Tansathien and P. Chaodumrong. 1992 An Introduction to Geology of Thailand, pp. 737-752**.** *In* **National Conference on Geologic Resources of Thailand: Potential for Future Development**. 17-24 November 1992, Department of Mineral Resources, Bangkok, Thailand.

Prasertying, A. 2008. **Rainfall pattern in landslide areas**. M.S. Thesis, Chulalongkorn University.

Robert, F.L. and A. W. Hatheway. 1988. **Geology and Engineering.** 3rd ed. McGrew-Hill Book Co., Singapore.

Schmidt, K.M., J.J. Roering, J.D. Stock, W.E. Dietrich, D.R. Montgomery and T. Schaub. 2001. The Variability of Root Cohesion as an Influence on Shallow Landslide Susceptibility in the Oregon Coast Range. **Canadian Geotechnical Journal** 38: 995 – 1024.

Silverman, B. A., S. A. Changnon Jr., J. A. Flueck, and S. F. Lintner. 1986. **Weather modification assessment: Kingdom of Thailand.** U.S.Department of Interior, Bureau of Reclamation Technical Report, USA.

Smith, G.D. 2003. **Numerical Solution of Partial Differential Equations.** Oxford University press, United Kingdom.

Soralump, S. and W. Chotikasathien. 2007. Integration of geotechnical engineering and rainfall data into landslide hazard map in Thailand, pp. 125 – 131. *In* **GEOTHAI'07 International Conference on Geology of Thailand: Towards Sustainable Development and Sufficiency Economy.** 21-22 December 2007, Department of Mineral Resources , Bangkok.

Tangtam, N, P. Narangjavana, P. Dhanmanonda, S. Boonyawat, C. Yarwudhi, W. Arunpraparut, P. Saguantam and V. Udomchoke. 1994. **Risk Area Classification for Flood and Natural Hazards in Southern Watersheds.** Kasetsart University and Office of Natural Resources and Environmental Policy and Planning.

The National Center for Atmospheric Research. 2006. **Weather Forecast Accuracy Gets Boost with New Computer Model.** Available Source: http://www.ucar.edu/news/releases/2006/wrf.shtml, 27 June 2010.

Thiebes B., R. Bell and T. Glade. 2007. Deterministic landslide susceptibility analysis using SINMAP - a case study in the Swabian Alb, pp. 177 – 184. *In* **Proceedings of the Conference 'Geomorphology for the Future'**, 26-28 July 2007. Obergurgl, Austria.

Thomson, G. R. and J. Turk. 2007. **Earth Science and Environment.** 4th ed. Thomson Learning Inc, Canada.

Udomchoke. V. 1981. **Pore-size Distribution of Hill-evergreen Forest Soil and Shifting Cultivated Soil at Doi Pui, Chiang Mai Province, Thailand.** M.S. Thesis, Kasetsart University.

Udomchoke. V. and O. Mingthipol. 1995. The Environmental Geology of the Low-Hill Watershed at Huai Jo, Chaing Mai Basin. **KU Science Journal** 13: 16-35.

Udomchoke, V., U. Homchan, P. Booppha, N. Youngthanissara, T. Rerkmaneewan, K. Kitikard, K. Kesjinda, S. Phanuthai and C. Sritulanon. 2010. **Landslides Disaster Prediction and Warning System from Heavy Raining Condition at Head Watershed of Chiang Dao District, Chiang Mai Province**. Nation Research Council (NRC), Thailand.

Varnes, D. J. 1984. Landslide Hazard Zonation: a review of principles and practice**,** **Natural Hazards** 3: 63.

APPENDIX

Appendix Table 1 Texture of soil profile, aspect, slope and elevation at eighteen soil sampling station at Mae Mhae watershed.

Name	Easting	Northing	Elevation	Aspect	Slope (%)	Profile	Depth (cm)	Texture
X-01	485628.4	2136106.1	1023	SE	57	A	0 - 30	clay loam
						B	30 - 360	sandy clay loam
						C	> 360	sandy loam
X-02	483291.1	2137306.5	1345	E	22	A	0 - 55	clay loam
						B	55 - 600	sandy clay loam
						C	> 600	sandy loam
X-03	483221.7	2137164.9	1342	SE	71	A	0 - 37	clay loam
						B	37 - 360	sandy clay loam
						C	> 360	sandy loam
X-04	483278.3	2137058.6	1296	SE	71	A	0 - 30	clay loam
						B	30 - 360	sandy clay loam
						C	> 360	sandy loam
X-05	484080.2	2136396.2	1149	S	27	A	0 - 30	clay loam
						B	30 - 405	sandy clay loam
						C	> 405	sandy loam

Appendix Table 1 (Continued)

Name	Easting	Northing	Elevation	Aspect	Slope (%)	Profile	Depth (cm)	Texture
X-06	484131.7	2136405.0	1155	S	31	A	0 - 30	clay loam
						B	30 - 405	sandy clay loam
						C	> 405	sandy loam
X-07	484405.7	2136142.5	1140	SW	9	A	0 - 32	clay loam
						B	32 - 450	sandy clay loam
						C	> 450	sandy loam
X-08	485065.6	2133872.5	1352	E	218	A	0 - 32	clay loam
						B	32 - 420	sandy clay loam
						C	> 420	sandy loam
X-09	485061.6	2134092.7	1301	NE	58	A	0 - 37	clay loam
						B	37 - 450	sandy clay loam
						C	> 480	sandy loam
X-10	486187.1	2135972.9	948	SE	62	A	0 - 30	clay loam
						B	30 - 360	sandy clay loam

Appendix Table 1 (Continued)

Name	Easting	Northing	Elevation	Aspect	Slope (%)	Profile	Depth (cm)	Texture
						C	> 360	sandy loam
X-11	487269.9	2135608.0	975	NE	43	A	0 - 45	clay loam
						B	45 - 540	sandy clay loam
						C	> 540	sandy loam
X-12	489456.5	2136371.2	718	E	67	A	0 - 34	clay loam
						B	34 - 480	sandy clay loam
						C	> 480	sandy loam
X-13	492005.0	2136626.7	522	E	37	A	0 - 34	clay loam
						B	34 - 522	sandy clay loam
						C	> 522	sandy loam
X-14	487658.2	2138099.7	867	S	72	A	0 - 30	clay loam
						B	30 - 315	sandy clay loam
						C	> 315	sandy loam

Appendix Table 1 (Continued)

Name	Easting	Northing	Elevation	Aspect	Slope (%)	Profile	Depth (cm)	Texture
X-15	487531.2	2138136.3	873	S	41	A	0 - 32	clay loam
						B	32 - 360	sandy clay loam
						C	> 360	sandy loam
X-16	487134.0	2138036.9	898	S	45	A	0 - 29	clay loam
						B	29 - 360	sandy clay loam
						C	> 360	sandy loam
X-17	486269.2	2138840.9	1009	S	21	A	0 - 32	clay loam
						B	32 - 405	sandy clay loam
						C	> 405	sandy loam
X-18	490533.8	2135551.8	648	E	53	A	0 - 34	clay loam
						B	34 - 420	sandy clay loam
						C	> 420	sandy loam

Appendix Table 2 Soil moisture content for initial API value on Mar, 3rd 2011 during no rain for long duration.

Station	Location	Depth (cm)	Weight of Soil (g)		Soil moisture (% by weight)
			Wet soil	Dry soil	
Ban Pang Hong 1	E 487867 N 2137781	10	76.39	66.97	14.07
		100	93.42	82.29	13.53
		130	94.37	82.45	14.46
		230	75.72	67.29	12.53
Ban Pang Hong 2	E 486753 N 2138853	10	81.84	70.28	16.45
		100	85.66	77.89	9.98
		130	74.01	68.25	8.44
		200	89.75	82.86	8.32
Ban Pang Hong 3	E 485501 N 2139211	10	86.26	76.64	12.55
		100	95.22	84.29	12.97
		130	86.77	78.39	10.69
		300	94.84	85.8	10.54
Ban Mae Mhae 1	E 489374 N 2136373	10	82.3	74.25	10.84
		100	101.44	91.15	11.29
		130	89.2	80.3	11.08
		230	80.68	73.57	9.66
Ban Mae Mhae 2	E 487054 N 2135529	10	84.06	71.83	17.03
		100	98.07	85.16	15.16
		130	100.01	87.6	14.17
		260	83.89	73.5	14.14

Appendix Table 2 (Continued)

Station	Location	Depth (cm	Weight of Soil (g)		Soil moisture (% by weight)
			Wet soil	Dry soil	
Ban Mae Mhae 3	E 483378 N 2136913	10	89.54	81.38	10.03
		100	100.4	91.82	9.34
		130	83.52	76.27	9.51
		240	88.12	80.12	9.99
Huai Mae Sai 1	E 489597 N 2135410	10	70	62.88	11.32
		100	75.77	67	13.09
		130	89.76	81.21	10.53
		260	80.67	74.84	7.79
Huai Mae Sai 2	E 489488 N 2134932	10	90.01	80.65	11.61
		100	90.62	76.81	17.98
		130	79.58	71.69	11.01
		260	78.99	70.43	12.15
Huai Mae Sai 3	E 489499 N 2133526	10	87.92	74.2	18.49
		100	86.46	72.63	19.04
		130	83.8	72.71	15.25
		240	90.75	79.48	14.18

Appendix Table 3 Runoff Curve Number.

Description of Land Use	Hydrologic Soil Group			
	A	B	C	D
Paved parking lots, roofs, driveways	98	98	98	98
Streets and Roads:				
Paved with curbs and storm sewers	98	98	98	98
Gravel	76	85	89	91
Dirt	72	82	87	89
Cultivated (Agricultural Crop) Land*:				
Without conservation treatment (no terraces)	72	81	88	91
With conservation treatment (terraces, contours)	62	71	78	81
Poor (<50% ground cover or heavily grazed)	68	79	86	89

Appendix Table 3 (Continued)

Description of Land Use	Hydrologic Soil Group			
	A	B	C	D
Pasture or Range Land:				
Good (50-75% ground cover; not heavily grazed)	39	61	74	80
Meadow (grass, no grazing, mowed for hay)	30	58	71	78
Brush (good, >75% ground cover)	30	48	65	73
Woods and Forests:				
Poor (small trees/brush destroyed by over-grazing or burning)	45	66	77	83
Fair (grazing but not burned; some brush)	36	60	73	79
Good (no grazing; brush covers ground)	30	55	70	77
Open Spaces (lawns, parks, golf courses, cemeteries, etc.)				

Appendix Table 3 (Continued)

Description of Land Use	Hydrologic Soil Group			
	A	B	C	D
Fair (grass covers 50-75% of area)	49	69	79	84
Good (grass covers >75% of area)	39	61	74	80
Commercial and Business Districts (85% impervious)	89	92	94	95
Industrial Districts (72% impervious)	81	88	91	93
Residential Areas:				
1/8 Acre lots, about 65% impervious	77	85	90	92
1/4 Acre lots, about 38% impervious	61	75	83	87
1/2 Acre lots, about 25% impervious	54	70	80	85
1 Acre lots, about 20% impervious	51	68	79	84

Source : Chow *et al.* (1988)

Appendix Table 4 Antecedent Precipitation Index from Curve Number of soil profile.

Location	Depth	Date												
		6/5/10	13/5/10	25/5/10	15/6/10	25/6/10	9/7/10	23/7/10	9/8/10	24/8/10	7/9/10	21/9/10	15/10/10	26/10/10
Huai Mae Sai	0 - 15	9.64	11.32	16.59	24.44	36.17	66.63	37.00	42.80	42.18	37.52	40.98	40.55	45.22
	15 - 35	14.44	19.50	34.33	36.07	58.41	47.11	55.75	60.72	57.53	55.81	65.34	65.38	73.45
	35 - 55	15.17	20.66	29.06	41.39	67.98	44.59	61.63	69.09	70.52	58.16	64.04	75.04	74.92
	55 - 100	36.73	42.97	83.92	92.00	115.58	101.28	138.13	146.62	158.08	136.71	155.16	176.00	180.36
Ban Mae Mhae	0 - 15	33.10	11.66	23.23	37.76	45.87	48.06	33.17	45.06	47.17	48.38	43.58	62.10	56.44
	15 - 35	43.69	36.24	45.64	51.27	63.10	59.26	61.57	61.93	68.90	61.25	89.58	65.24	76.11
	35 - 55	32.16	32.10	39.07	47.22	63.01	55.25	60.29	60.04	61.80	55.65	68.34	71.32	67.44
	55 - 100	45.02	77.11	114.15	135.20	149.86	132.09	141.02	136.81	138.32	137.24	118.04	157.24	155.03
Ban Pang Mai	0 - 15	26.95	15.33	42.50	28.96	50.66	46.26	39.78	46.54	53.16	55.21	47.77	54.48	56.90
	15 - 35	33.89	26.33	50.26	32.52	56.02	55.70	48.45	53.17	51.69	52.33	49.61	62.26	59.60
	35 - 55	48.64	36.08	60.16	48.25	68.09	64.19	69.43	67.69	76.87	64.89	71.39	74.83	65.53
	55 - 100	78.65	92.47	127.86	97.98	153.21	171.59	130.50	153.88	159.53	150.14	152.82	164.44	157.99

Appendix Table 5 Antecedent Precipitation Index from Weather Research Forecasting.

Location	Depth	Date												
		6/5/10	13/5/10	25/5/10	15/6/10	25/6/10	9/7/10	23/7/10	9/8/10	24/8/10	7/9/10	21/9/10	15/10/10	26/10/10
Huai Mae Sai	0 - 10	10.56	11.03	23.39	21.28	26.04	27.47	30.88	32.34	30.80	32.60	31.84	30.93	30.04
	10 - 40	31.69	33.10	70.17	63.83	78.13	82.42	92.65	97.03	92.41	97.80	95.53	92.78	90.12
	40 - 100	75.02	73.24	81.73	99.14	111.10	156.36	152.22	195.34	192.29	204.16	197.43	185.82	190.20
	100 - 200	211.49	211.49	212.52	219.78	224.89	241.35	258.95	304.14	333.33	361.71	351.34	326.19	308.42
Ban Mae Mhae	0 - 10	10.56	10.95	23.36	21.46	26.20	27.58	31.04	33.03	31.49	33.27	32.40	31.35	30.38
	10 - 40	31.68	32.85	70.07	64.38	78.59	82.73	93.12	99.10	94.47	99.81	97.21	94.06	91.13
	40 - 100	74.95	73.18	81.42	99.43	111.71	157.25	153.16	199.93	196.69	208.63	201.43	189.40	192.88
	100 - 200	211.64	211.64	212.66	219.87	224.98	241.76	259.69	306.20	336.18	365.35	354.29	327.93	311.77
Ban Pang Mai	0 - 10	10.74	11.55	23.78	21.77	26.24	27.77	31.23	32.27	30.88	32.57	31.86	30.96	30.18
	10 - 40	32.21	34.66	71.34	65.32	78.73	83.32	93.69	96.82	92.65	97.71	95.59	92.87	90.53
	40 - 100	76.56	74.85	84.01	101.59	113.59	157.72	154.06	194.34	191.76	203.64	197.22	185.95	190.70
	100 - 200	210.82	210.82	211.93	219.77	225.24	242.11	260.58	302.32	330.96	359.37	349.70	325.62	309.62

Appendix Table 6 Field direct shear testing with 3 load at Huai Mae Sai.

Load 50 kg					Load 73 kg					Load 133 kg				
Proving ring reading	shear force	Dial guage reading	stress	strain	Proving ring reading	shear force	Dial guage reading	stress	strain	Proving ring reading	shear force	Dial guage reading	stress	strain
0	0	116	0	0.0041	0	0	102	0	0.00364	0	0	209	0	0.0075
10	119.7	133	1526.6	0.0048	10	119.7	110	1526.6	0.00393	10	119.7	218	1526.6	0.0078
15	179.5	144	2289.8	0.0051	15	179.5	115	2289.8	0.00411	20	239.4	223	3053.1	0.0080
20	239.4	154	3053.1	0.0055	20	239.4	120	3053.1	0.00429	30	359.0	230	4579.7	0.0082
25	299.2	168	3816.4	0.0060	25	299.2	130	3816.4	0.00464	40	478.7	238	6106.2	0.0085
30	359.0	197	4579.7	0.0070	30	359.0	140	4579.7	0.00500	50	598.4	246	7632.8	0.0088
35	418.9	220	5342.9	0.0079	35	418.9	154	5342.9	0.00550	60	718.1	255	9159.3	0.0091
40	478.7	255	6106.2	0.0091	40	478.7	180	6106.2	0.00643	70	837.8	270	10685.9	0.0096
45	538.6	190	6869.5	0.0068	45	538.6	208	6869.5	0.00743	80	957.5	288	12212.4	0.0103
50	598.4	328	7632.8	0.0117	50	598.4	230	7632.8	0.00821	90	1077.1	310	13739.0	0.0111
55	658.3	375	8396.1	0.0134	55	658.3	257	8396.1	0.00918	93	1113.0	325	14197.0	0.0116
60	718.1	435	9159.3	0.0155	60	718.1	283	9159.3	0.01011	98	1172.9	350	14960.3	0.0125
65	777.9	480	9922.6	0.0171	65	777.9	327	9922.6	0.01168	103	1232.7	385	15723.5	0.0138
70	837.8	538	10685.9	0.0192	70	837.8	370	10685.9	0.01321	108	1292.6	410	16486.8	0.0146

Appendix Table 6 (Continued)

Load 50 kg					Load 73 kg					Load 133 kg				
Proving ring reading	shear force	Dial guage reading	stress	strain	Proving ring reading		Dial guage reading	stress	strain	Proving ring reading		Dial guage reading	stress	strain
75	897.6	617	11449.2	0.0220	75	897.6	425	11449.2	0.01518	113	1352.4	460	17250.1	0.0164
80	957.5	692	12212.4	0.0247	80	957.5	488	12212.4	0.01743	118	1412.2	522	18013.4	0.0186
85	1017.3	760	12975.7	0.0271	85	1017.3	527	12975.7	0.01882	123	1472.1	555	18776.6	0.0198
90	1077.1	820	13739.0	0.0293	90	1077.1	580	13739.0	0.02071	128	1531.9	600	19539.9	0.0214
					95	1137.0	642	14502.3	0.02293	133	1591.8	660	20303.2	0.0236
										138	1651.6	740	21066.5	0.0264
										143	1711.5	805	21829.8	0.0288
										148	1771.3	860	22593.0	0.0307
										153	1831.1	925	23356.3	0.0330
										158	1891.0	1020	24119.6	0.0364

Appendix Table 7 Field direct shear testing with 3 load at Huai Mae Mhae.

Load 50 kg					Load 73 kg					Load 133 kg				
Proving ring reading	shear force	Dial guage reading	stress	strain	Proving ring reading		Dial guage reading	stress	strain	Proving ring reading		Dial guage reading	stress	strain
0	0	290	0	0.01036	0	0	320	0	0.01143	0	0	127	0	0.00454
10	119.7	296	1526.6	0.01057	10	119.7	325	1526.6	0.01161	10	119.7	129	1526.6	0.00461
20	239.4	300	3053.1	0.01071	20	239.4	337	3053.1	0.01204	20	239.4	130	3053.1	0.00464
30	359.0	316	4579.7	0.01129	30	359.0	358	4579.7	0.01279	30	359.0	138	4579.7	0.00493
40	478.7	348	6106.2	0.01243	40	478.7	408	6106.2	0.01457	40	478.7	148	6106.2	0.00529
50	598.4	385	7632.8	0.01375	50	598.4	565	7632.8	0.02018	50	598.4	156	7632.8	0.00557
60	718.1	445	9159.3	0.01589	52	622.3	630	7938.1	0.02250	60	718.1	170	9159.3	0.00607
70	837.8	552	10685.9	0.01971						70	837.8	182	10685.9	0.00650
73	873.7	650	11143.9	0.02321						80	957.5	204	12212.4	0.00729
										90	1077.1	300	13739.0	0.01071
										93	1113.0	330	14197.0	0.01179

Appendix Table 8 Physical properties of mountainous soil from granite host rock in the Northern Thailand.

sample number	soil type	Gradation (% passing sieve)				Atterberg limits			Gs	unconsolidated undrain triaxial test	ϕ
		#4	#10	#40	#200	LL (%)	PL (%)	PI (%)		cohesion (ton m^{-2})	(degree)
KL-1	clayey sand	-	-	-	-	-	-	-	2.73	3.0	20.0
	clayey sand	-	-	-	-	-	-	-	2.74	2.7	17.2
KL-2	sandy clay trace gravel	96	78	62	55	56	27	28	2.72	2.6	25.4
	sandy clay trace gravel	96	77	61	53	59	24	34	2.72	3.0	25.0
KL-3	clayey sand trace gravel	-	-	-	-	-	-	-	2.73	4.9	22.5
	sandy clay trace gravel	-	-	-	-	-	-	-	2.72	6.4	19.7
RM-1	clayey fine to medium sand	-	-	-	-	-	-	-	2.71	2.6	18.0
	silty fine sand	-	-	-	-	-	-	-	2.71	1.6	22.0
RM-2	fine to medium sandy clay	99	91	72	64	64	27	37	2.71	5.0	26.6
	silty with fine sand	100	94	68	57	42	30	11	2.74	2.7	20.0
RM-3	silty fine to medium sandy clay	-	-	-	-	-	-	-	2.71	5.6	27.2
	silty fine to medium sandy clay	-	-	-	-	-	-	-	2.72	3.0	28.0
HK-1	clayey sand trace gravel	-	-	-	-	-	-	-	2.67	1.6	25.4
	clayey sand trace gravel	-	-	-	-	-	-	-	2.67	5.0	30.0
HK-2	clayey sand with gravel	85	53	37	30	43	22	21	2.67	2.0	23.8
	clayey sandy gravel	62	44	30	25	38	18	20	2.68	3.4	23.2
HK-3	clay with sand trace gravel	-	-	-	-	-	-	-	2.70	5.5	22.0
STP-1	sandy clay	-	-	-	-	-	-	-	2.67	6.0	15.2
STP-3	clay with sand	-	-	-	-	-	-	-	2.633	2.8	26.5

Appendix Table 8 (Continued)

sample number	soil type	Gradation (% passing sieve)				Atterberg limits			Gs	unconsolidated undrain triaxial test	ϕ
		#4	#10	#40	#200	LL (%)	PL (%)	PI (%)		cohesion (ton m^{-2})	(degree)
NT-1	silty fine to medium sand	-	-	-	-	-	-	-	2.682	1.0	37.5
NT-2	silty fine to medium sand	-	96	50	25	nonplastic			2.674	0.5	40.2
NT-3	clayey fine to medium sand	-	-	-	-	-	-	-	2.712	1.0	32.0
LS-1	sandy clay trace gravel	-	-	-	-	-	-	-	2.665	2.8	21.0
	sandy clay trace gravel	-	-	-	-	-	-	-	2.678	3.0	29.5
LS-2	clayey fine to medium sand trace gravel	98	94	63	49	51	21	30	2.673	2.1	17.0
	clayey sand with gravel	86	69	48	41	61	24	37	2.684	1.4	25.1
LS-3	sandy clay	-	-	-	-	-	-	-	2.661	4.5	20.1
	clayey fine to medium sand trace gravel	-	-	-	-	-	-	-	2.694	4.4	22.5
PP-1	silty clayey sand trace gravel	-	-	-	-	-	-	-	2.656	4.3	30.2
	silty sandy clay trace gravel	-	-	-	-	-	-	-	2.662	4.3	18.1
PP-2	clayey sand trace gravel	92	60	49	47	67	28	38	2.678	6.0	17.5
	clayey sand trace gravel	84	61	52	48	60	29	31	2.665	3.3	26.8
PP-3	silty sandy clay	-	-	-	-	-	-	-	2.676	3.0	14.3
	silty clayey sand	-	-	-	-	-	-	-	2.693	1.5	21.5

Appendix Table 8 (Continued)

sample number	soil type	Gradation (% passing sieve)				Atterberg limits			Gs	unconsolidated undrain triaxial test	ϕ
		#4	#10	#40	#200	LL (%)	PL (%)	PI (%)		cohesion (ton m^{-2})	(degree)
NT-1	silty fine to medium sand	-	-	-	-	-	-	-	2.682	1.0	37.5
NT-2	silty fine to medium sand	-	96	50	25	nonplastic			2.674	0.5	40.2
NT-3	clayey fine to medium sand	-	-	-	-	-	-	-	2.712	1.0	32.0
LS-1	sandy clay trace gravel	-	-	-	-	-	-	-	2.665	2.8	21.0
	sandy clay trace gravel	-	-	-	-	-	-	-	2.678	3.0	29.5
LS-2	clayey fine to medium sand trace gravel	98	94	63	49	51	21	30	2.673	2.1	17.0
	clayey sand with gravel	86	69	48	41	61	24	37	2.684	1.4	25.1
LS-3	sandy clay	-	-	-	-	-	-	-	2.661	4.5	20.1
	clayey fine to medium sand trace gravel	-	-	-	-	-	-	-	2.694	4.4	22.5
PP-1	silty clayey sand trace gravel	-	-	-	-	-	-	-	2.656	4.3	30.2
	silty sandy clay trace gravel	-	-	-	-	-	-	-	2.662	4.3	18.1
PP-2	clayey sand trace gravel	92	60	49	47	67	28	38	2.678	6.0	17.5
	clayey sand trace gravel	84	61	52	48	60	29	31	2.665	3.3	26.8
PP-3	silty sandy clay	-	-	-	-	-	-	-	2.676	3.0	14.3
	silty clayey sand	-	-	-	-	-	-	-	2.693	1.5	21.5

Source: Department of Water Resources (2005)

Appendix Table 9 Morphologic characteristics of landslides and pits with associated root attributes in different vegetation communities.

Basal area (m^2)	Lateral area (m^2)	Median depth (m)	Landslide perimeter (m)	Landslide volume (m^3)	Slope (degree)	No. of roots	Lateral root cohesion (kPa)	Tensile force ($kg \cdot m\ s^{-2}$, $\times 10^3$)	Median root depth (m)	A/b (m)	A/b sin (slope) (m)	Time since disturbance (years)
Natural Forest Pit												
-	2.12	1.25	-	-	34	351	151.9	321.5	0.40	50	89	300
-	1.92	0.94	-	-	34	355	94.3	181.5	0.12	3482	6227	300
-	2.15	1.46	-	-	34	247	50.8	105.5	0.30	3122	5583	300
							94.3					
Natural Forest Landslide												
59.1	26.78	0.83	24.5	49.1	38	237	11.0	322.1	0.37	1250	2030	200
Inferred Natural Forest												
132.0	15.40	0.70	20.5	92.4	37	95	58.8	904.9	0.20	1171	1946	300
75.0	16.42	0.71	18.5	53.3	39	507	83.9	1377.1	0.15	22031	3227	300
							71.4					
Natural Forest Blowdown Landslide												
42.0	75.52	0.82	71.8	34.4	43	514	33.4	2525.1	0.38	43	63	200
30.9	17.81	0.58	27.6	17.9	39	656	17.8	316.4	0.20	140	222	300
							25.6					
Industrial Forest Pit												
-	3.46	1.30	-	-	32	425	36.5	85.9	0.40	798	1506	100(30)
-	2.74	0.88	-	-	35	96	9.8	24.9	0.20	570	994	100(30)
							23.2					

Appendix Table 9 (Continued)

Basal area (m^2)	Lateral area (m^2)	Median depth (m)	Landslide perimeter (m)	Landslide volume (m^3)	Slope (degree)	No. of roots	Lateral root cohesion (kPa)	Tensile force ($kg \cdot m\ s^{-2}$, $\times 10^3$)	Median root depth (m)	A/b (m)	A/b sin (slope) (m)	Time since disturbance (years)
Industrial Forest Landslide												
Elliot State Forest (ESF)												
72.2	21.75	1.07	22.5	77.3	44	100	4.2	90.5	0.10	22	32	109
31.6	13.07	0.74	15.2	23.4	46	780	3.8	49.3	0.15	125	174	103
7.4	1.29	0.16	8	1.2	44	947	2.8	2.9	0.15	111	160	103
14.4	4.31	0.48	12.7	6.9	47	628	2.8	12.0	0.15	104	142	103
34.0	27.40	1.64	18.0	55.8	40	536	12.1	330.3	0.20	244	379	96
44.9	26.96	1.19	17.7	53.4	43	1291	8.3	222.4	0.10	500	733	96
-	6.61	0.67	-	-	43	355	1.8	12.2	0.10	500	733	96
-	5.54	1.28	-	-	43	138	10.9	60.2	0.05	500	733	96
11.4	11.30	1.02	11.0	11.7	45	2207	6.9	78.2	0.10	1029	1455	103
5.6	3.23	0.62	4.9	3.5	34	1050	8.8	28.6	0.10	1596	2854	103
40.2	31.27	1.09	25.4	43.8	32	563	3.5	108.2	0.10	1596	3012	100
Cut-boundary												
179.2	19.44	0.51	45.8	91.4	42	2922	8.9	183.1	0.20	20	30	109
Mapleton District												
35.8	14.29	0.65	17.3	23.2	44	245	21.3	304.1	0.38	222	320	43
51.3	21.86	0.72	24.5	36.9	43	617	6.6	144.5	0.28	233	342	123
							6.8					

Source: Schmidt *et al.* (2001)

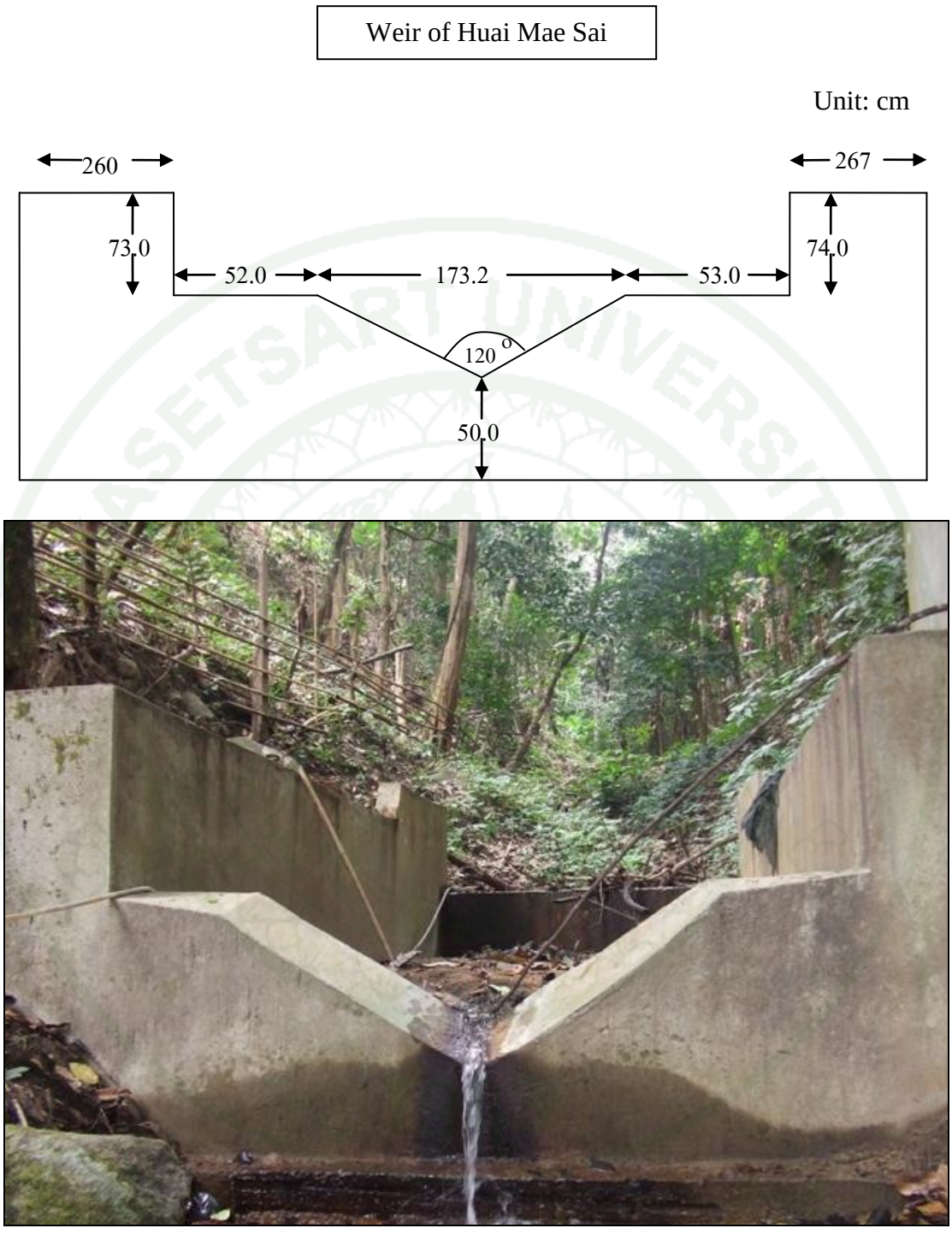

Appendix Figure 1 General Drawing of Mae Sai Weir (top) and picture of weir (below) at the outlet of Huai Mae Sai.

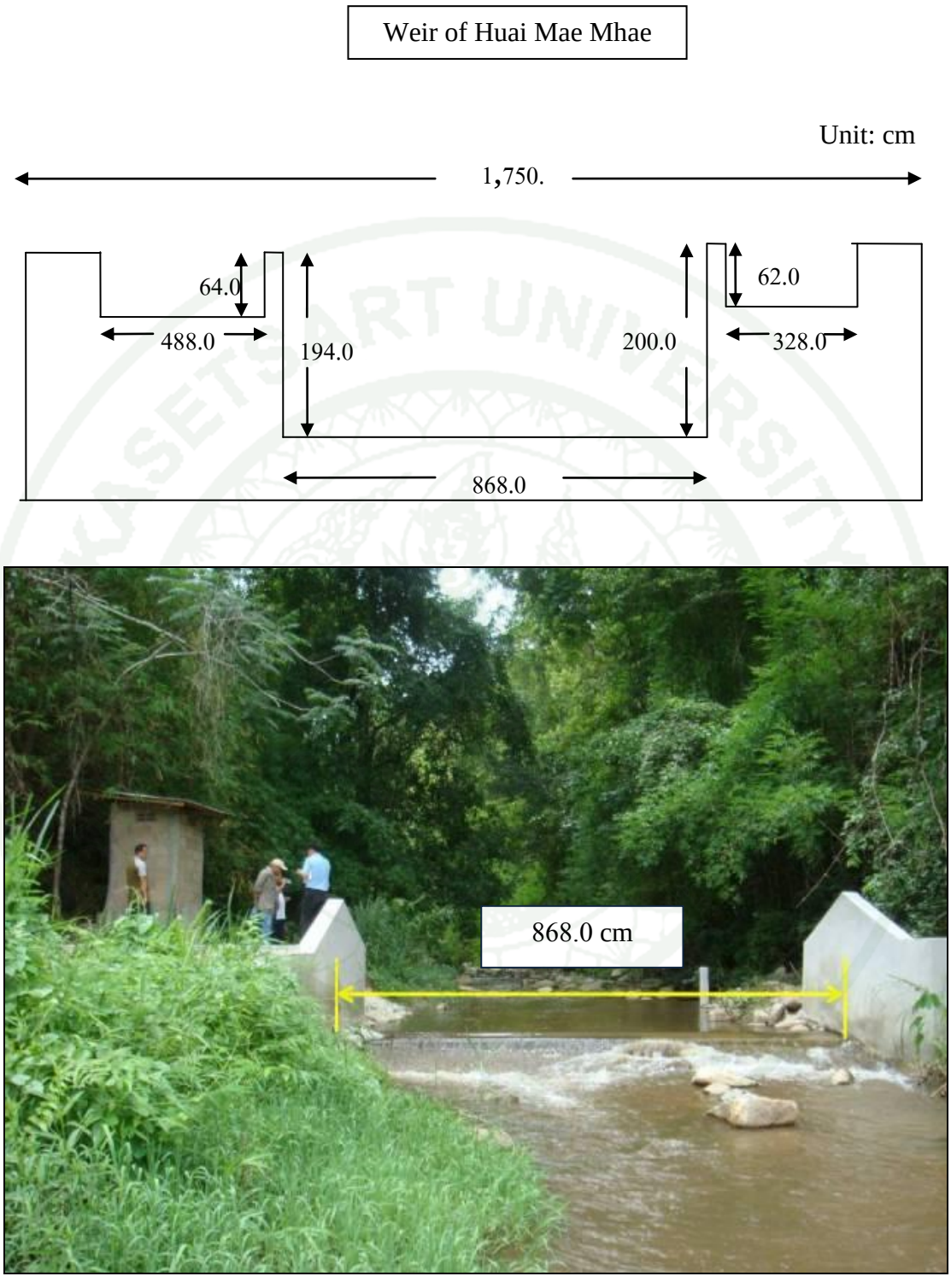

Appendix Figure 2 General Drawing of Mae Sai Weir (top) and picture of weir (below) at the outlet of Huai Mae Sai.

Appendix Figure 3 Undisturbed soil sampling for testing in laboratory**.**

Appendix Figure 4 Disturbed soil sampling for testing in laboratory**.**

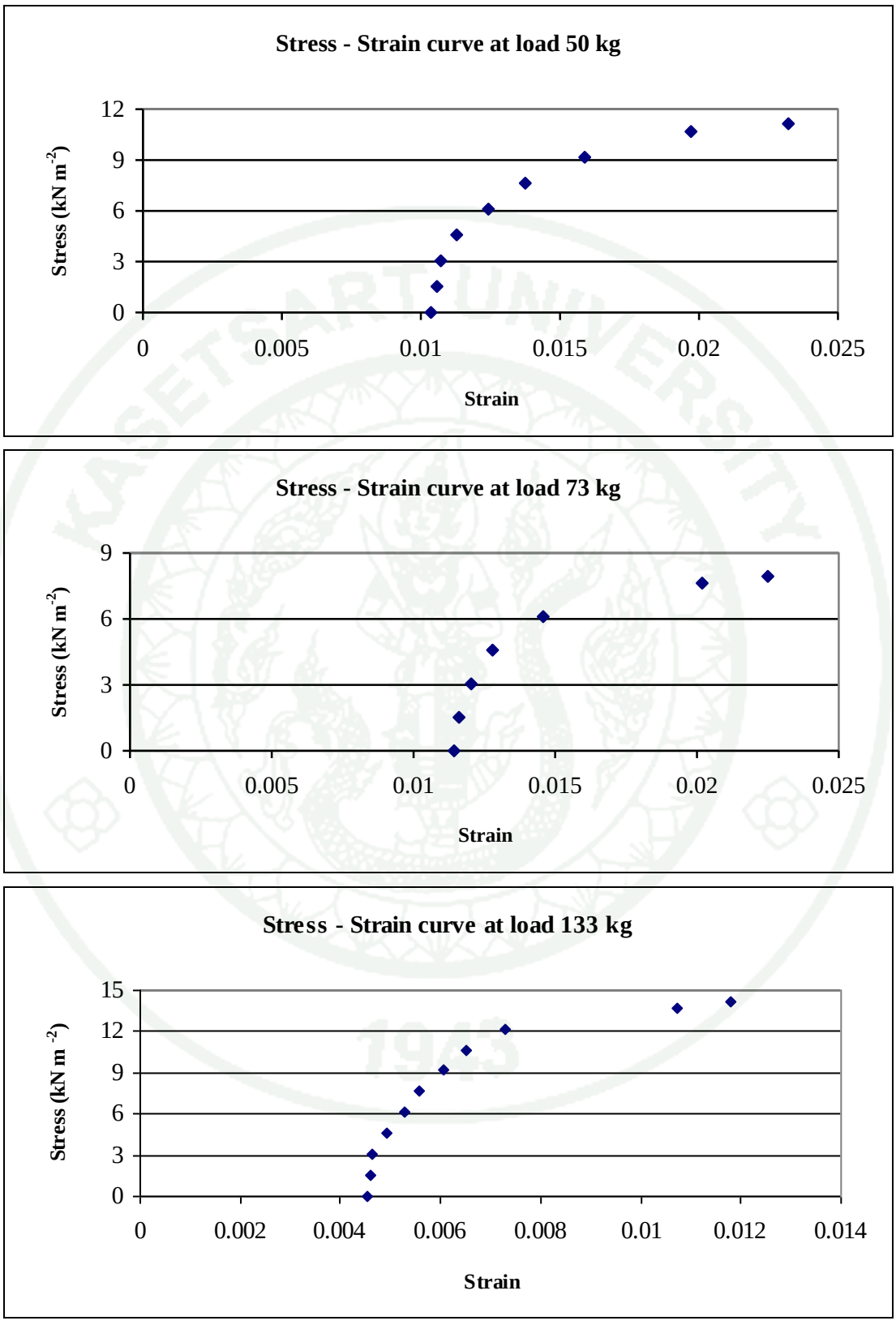

Appendix Figure 5 Stress and Strain curve of each load at Ban Mae Mhae**.**

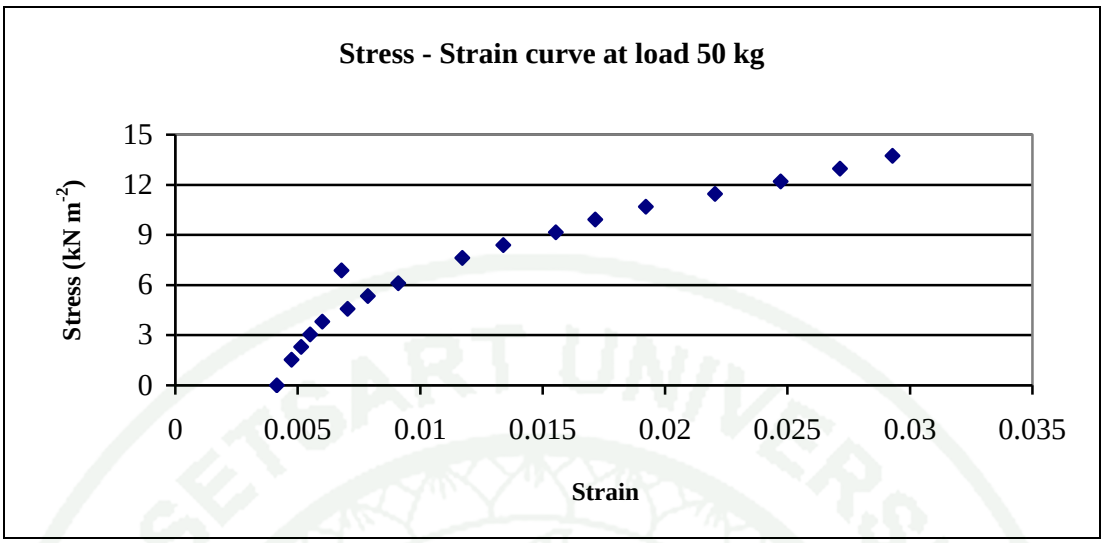

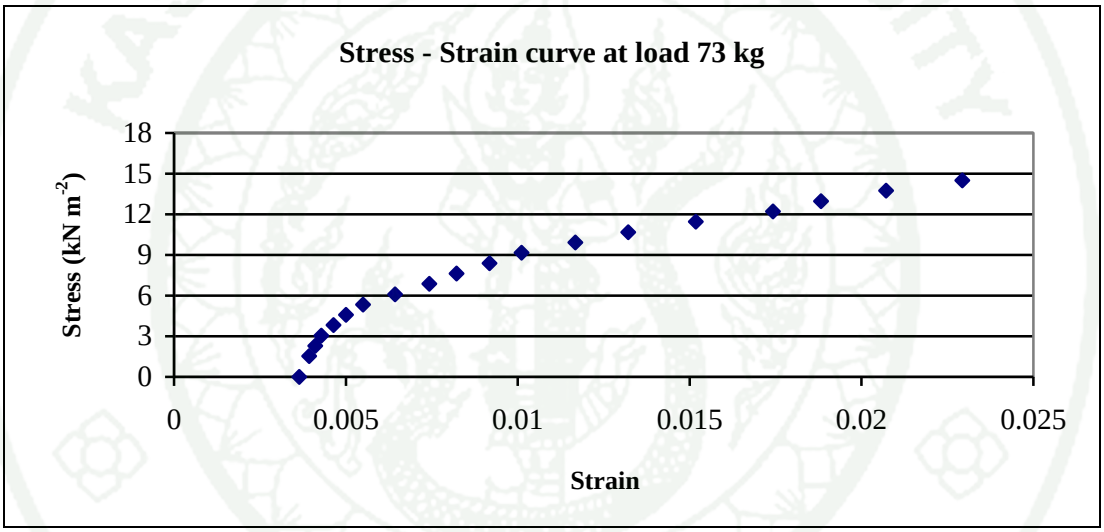

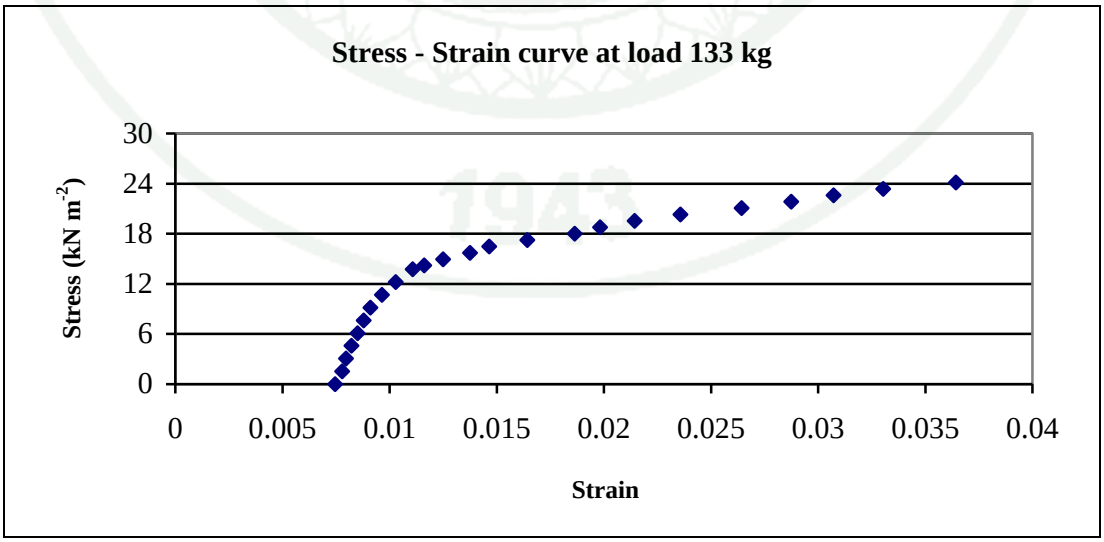

Appendix Figure 6 Stress and Strain curve of each load at Ban Mae Sai**.**

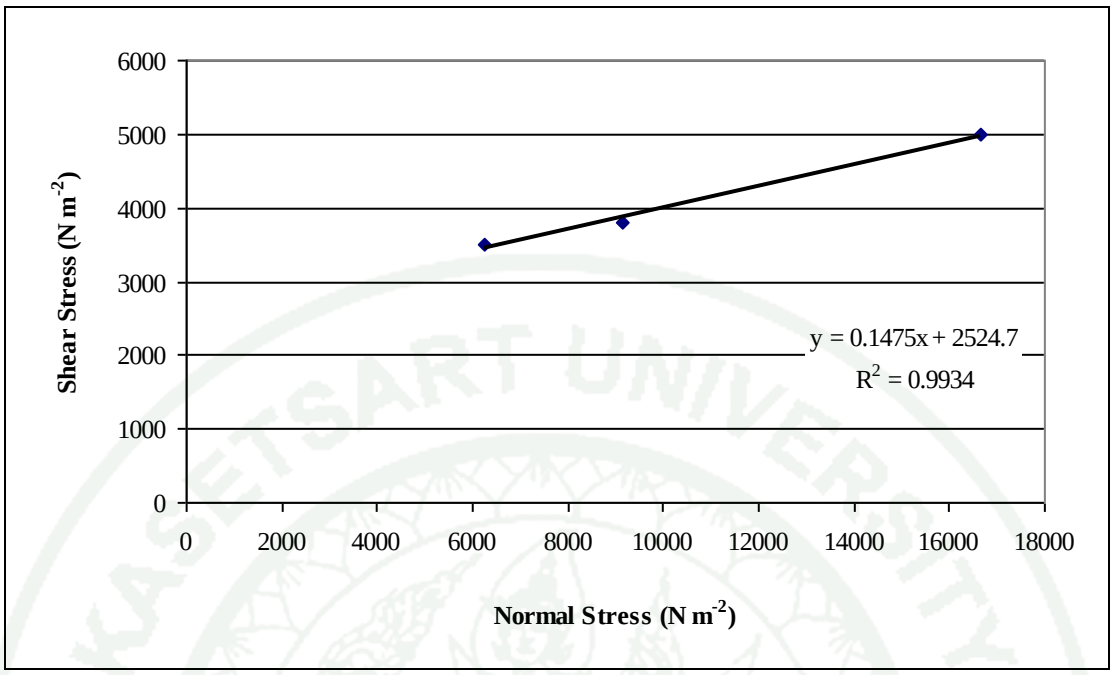

Appendix Figure 7 Normal stress and shear stress graph of Mae Sai watershed.

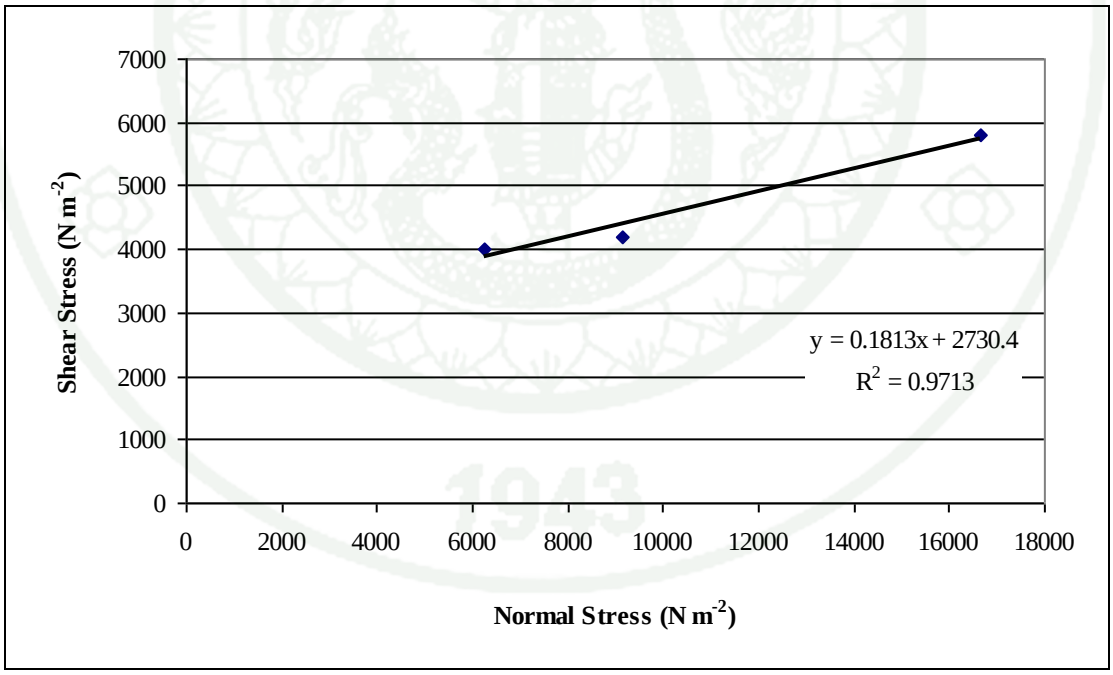

Appendix Figure 8 Normal stress and shear stress graph of Mae Mhae watershed.

CURRICULUM VITAE

NAME : Mr. Kamphol Kesjinda

BIRTH DATE : May 7, 1974

BIRTH PLACE : Bangkok, Thailand

EDUCATION : **YEAR** **INSTITUTE** **DEGREE/DIPLOMA**

1999 Chulalongkorn Univ. B.Eng (Survey Eng.)

POSITION/TITLE :

WORK PLACE : Faculty of Science, Kasetsart University

SCHOLARSHIP/AWARDS: Assistant Teaching Fund from Graduate School, Kasetsart University (2010)